中国人民大学本科毕业设计

二维晃动三角光晶格的拓扑性质研究

Topological Floquet States in Two-Dimensional Triangle Shaking Optical Lattice

作　　者:＿＿＿＿＿孙宁＿＿＿＿＿

学　　院:＿＿＿＿＿理学院＿＿＿＿

专　　业:＿＿＿＿＿物理学＿＿＿＿

年　　级:＿＿＿＿＿2011级＿＿＿＿

学　　号:＿＿＿2011201348＿＿＿

指导老师:＿＿＿＿＿翟荟＿＿＿＿＿

论文成绩:＿＿＿＿＿＿＿＿＿＿＿

日　　期:＿＿＿＿＿＿＿＿＿＿＿

Topological Floquet States in Two-Dimensional Triangle Shaking Optical Lattice

Ning Sun

May 13, 2015

摘　要

　　在这篇文章中，我们提出了一个夹角为三十度角的二维晃动三角光晶格的模型。我们简单回顾了描述这样一个周期含时驱动体系的Floquet理论及其有效哈密顿量。我们首先对静态光晶格进行了求解。通过数值对角化在布洛赫基矢下的截断哈密顿量矩阵，我们得到了静态晶格的能带以及布洛赫波函数。文中给出了由布洛赫波函数计算得到的实空间中在晶格格点局域化的万尼尔函数。通过上述得到的晶格能带与万尼尔波函数，可以构造最低两个能带的紧束缚近似模型。在做了旋转波近似后，文章给出了这个二维体系相应的有效哈密顿量。利用得到的有效哈密顿量，将可以对体系的拓扑性质进行研究，通过计算相关的拓扑量子数。二维体系中刻画拓扑性质的拓扑量子数是陈数。文章讨论了未来可能的展开计算体系陈数的方法，以及存在相应拓扑Floquet量子态的可能性。

关键词：　二维晃动光晶格　拓扑态　能带　万尼尔函数　有效哈密顿量

Abstract

In this article, we propose a scheme which could be able to realize topological Floquet states. Using shaking optical lattice, we construct a periodically driven system which could be analysed by Floquet theory. Floquet theory is briefly reviewed in the paper, as well as one efficient method to evaluate it, named Effective Hamiltonian. Our model is a two-dimensional shaking triangle optical lattice with intersection angle of $30°$ using shaking optical lattice. To study the shaking lattice, we firstly solve the static lattice. Energy bands as well as the Bloch functions are obtained by numerically diagonalization of the lattice Hamiltonian. Then the real-space-localized wave functions named Wannier functions are calculated by Fourier transform of the Bloch functions with respect to the quasi-momentum k. Using the Wannier functions obtained above we construct a Tight-bounding approximation model within the lowest two bands. After a Rotating-wave approximation, Effective Hamiltonian are given. We then discuss the possible way to characterize the topological properties of the system using some topological quantum numbers like Chern numbers. Possible methods for further calculating the Chern numbers of the system are also discussed as well. Topological nontrivial Floquet states might then be able to exist within some frames.

Keywords: two-dimensional triangle shaking optical lattice   topological Floquet states   energy bands   Wannier functions   Effective Hamiltonian

CONTENTS

LIST OF FIGURES

I. INTRODUCTION

I A . Background

The study of topological states has been one of the most interesting topic in condensed-matter physics in recent years [1,2]. Topological phase transition, as well as topological nontrivial quantum states have been extensively studied both theoretically and experimentally. With the discovery of new classes of materials called "topological insulators" in two- and three-dimensional systems [3–6], and the quantum anomalous Hall effect found in experiment [7], the effort of searching for nontrivial topological states in solid materials has been continuously growing.

In cold-atom physics, studying and realizing such topological states of matter is also one of the major trends nowadays. Cold-atom systems possess several advantages compared with the normal solid systems. Firstly, it is very clean. Whereas impurity always exists in solid matter systems, cold-atom system could be extremely purified, leading us to quite simplified models to describe it theoretically. It is also much more controllable that the interaction between atoms and external fields could be easily manipulated, so that the topological properties of quantum states can be engineered using standard experimental techniques. Experimentally, two main techniques developed in cold-atom systems are Raman laser coupling [8–15] and shaking optical lattice [16–18], both of which have been quite utilized for searching and studying topological quantum states. In addition, a wide range could the parameters of the system be manipulated through, which might be able to provide us new types of topological quantum states that without counterparts in solid systems.

In the past, topological characterization of periodically driven quantum systems have been theoretically studied [20–22] and a type of topological nontrivial quantum states named "Floquet Topological State" was proposed in such time-dependent systems. Such periodic time-dependent systems could be well analysed by Floquet theory [25], where "Floquet operators" are introduced to describe such a system. Since there are no well-defined ground states, unlike the cases of static (nondriven) systems, we instead classify the periodically driven systems in terms of the topological properties of their corresponding Floquet operators. One method to efficiently evaluate the Floquet operator in Floquet theory is by introducing an time-independent Effective Hamiltonian H_{eff} [27]. Besides, to discuss the topological properties, some topological quantum numbers are to be studied. Topological quantum numbers are known to play a crucial part in characterizing the quantum phenomena in lower dimensions in solid-state systems. A typical example is the famous

quantum Hall effect which could be characterized by Chern numbers associated with the Berry phase connection [19]. Here for a Floquet operator, always the topological invariants as winding numbers are concerned. While when comes to an time-independent Effective Hamiltonian, topological quantum numbers like Chern numbers are still available to characterize the topological properties of the quantum states, and are still to be studied. Recently, topological Floquet states have been proposed in several periodically driven systems [23, 24]. And it has been realized experimentally the topological Haldane model with ultracold Fermions [26].

In this paper, we construct our model using shaking optical lattice to provide a periodically driven system. We consider a shaking two-dimensional triangle lattice with an intersection angle of $30°$, where harmonic shaking are added along directions of two lattice vectors with the same frequency and amplitude. Firstly, energy bands for static two-dimensional triangle lattice, with the Bloch functions accompanied, are given by numerically solving the eigen-problem under a set of cut-off Bloch bases. Wannier functions localized in lattice site in real space are then obtained from Fourier transform of the Bloch functions with respect to the quasi-momentum k. Using the Wannier functions, a tight-bounding approximation model could be built then within the lowest two bands. And after a Rotating Wave Approximation transform, Effective Hamiltonian of the system could be calculated. For further study, Chern numbers are to be calculated using the results above.

To clarify, we plot the lowest several energy bands for a series of different values of potential depth of the lattice, from quite a small value approximate to zero to a very large value compared with the free particle energy (Figure 4-8). Wannier functions are also shown in Figure 9 and Figure 10, from which we see the functions are well localized in real space as expected.

I B . Outline of the Paper

The paper is structured as follow. In Sec. II, we construct our basic model of two-dimensional shaking triangle lattice with intersection angle of $30°$. Floquet theory and the Effective-Hamiltonian methods for studying time-dependent problems are briefly reviewed as well. Then in Sec. III, we present the process of solving the static triangle lattice, which makes a basic part of the solution of shaking triangle lattice. In this section, the energy bands are given, as well as the Wannier functions obtained straightforward from Fourier transform of the Bloch functions. In Sec. IV, we firstly construct the Tight Bounding Approximation model within the lowest two bands using the Wannier functions we obtained in Sec. III. Then Effective Hamiltonian are given. For future studying, we

discuss in Sec. V the possible way to calculate the Chern numbers of this system using the Effective Hamiltonian obtained in above for further study of the topological properties of the Floquet states.

In addition, some details of deduction of Effective Hamiltonian for Floquet operators are presented in Appendix A. Program code ever used in this work are presented in Appendix B.

II. TWO-DIMENSIONAL SHAKING OPTICAL LATTICE

The potential given by a general optical lattice performs like this

$$\mathcal{V}(r) = V[\cos(\vec{k} \cdot \vec{r})]^2$$

is equivalent to $V \cos(2\vec{k} \cdot \vec{r})$ by a trivial shift about the reference frame.

In the following, I choose the later form to clarify my work, that potential $\mathcal{V}(\vec{r})$ is in the form of $V \cos(2\vec{k} \cdot \vec{r})$.

II A . Setup

Consider a two-dimensional triangle optical lattice:

$$\mathcal{H} = T + \mathcal{V} = -\frac{\hbar^2}{2\mu} + V_1 \cos(2\vec{k_1} \cdot \vec{r_1}) + V_2 \cos(2\vec{k_2} \cdot \vec{r_2})$$

Here $\hat{r}_1 = \hat{e}_x$, $\hat{r}_2 = \cos(30°)\hat{e}_x - \sin(30°)\hat{e}_y$ represents the directions of two laser beams generating this two-dimensional triangle optical lattics.

Shaking was added along the directions of these two beams, giving a time-dependent Hamiltonian that

$$
\begin{aligned}
h(t) &= T + V(t) \\
&= \frac{p^2}{2\mu} - V_1 \cos(2\vec{k_1} \cdot \vec{r_1} + f_1 \cos(\omega_1 t)) - V_2 \cos(2\vec{k_2} \cdot \vec{r_2} + f_2 \cos(\omega_2 t + \alpha))
\end{aligned}
\tag{1}
$$

The general setup of this model is shown in Fig. 1 (Fig. 1a and Fig. 1b). A two-dimensional triangle lattice is formed with two lattices in two directions with an intersection angle of $30°$. Each lattice is produced by two counterpropagating lasers. Periodically modulating the relative phase between the two counterpropagating laser beams in each lattice, one can produce the shaking lattice describe by a time-dependent Hamiltonian in Eq.1.

To simplify, we consider only a simple case $f_1 = f_2$, $\omega_1 = \omega_2$ in the following, while generally α does not equal to zero. To fulfill this, one can modulate the time-dependent term in the same way[1] along the two directions of the lattices.

---

[1]By the same way, it means the same shaking amplitude and frequency.

(a) Setup of the two-dimensional triangle optical lattice with $30°$ intersection angle

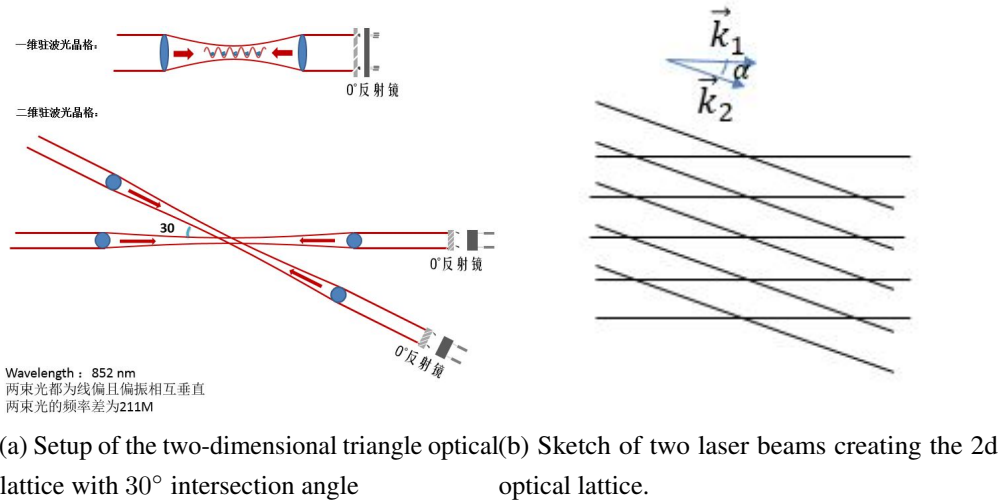(b) Sketch of two laser beams creating the 2d optical lattice.

Figure 1: Experimental Setup

II B . Shaking Lattice in Co-moving Frame of Reference

Noted that in the time-dependent Hamiltonian above, shaking effect is mixed with the space-periodic lattice effect. It is not a easy thing to solve such a time-dependent Hamiltonian directly. Meanwhile the intrinsic physics could not be obviously foreseen through it. However, by transferring to the co-moving frame of reference, $\vec{r} \to \vec{r} + \vec{\xi}(t)$, the Hamiltonian acquires a time-dependent vector potential term as $\dot{\vec{\xi}}(t) \cdot \vec{p}$. Another advantage is that the static lattice term is separated with shaking term, providing a way that we could make use of the clear results of static optical lattice straightforward. Thus we transfer the time-dependent Hamiltonian into co-moving frame of reference first.

Schrödinger equation reads

$$h(t) - i\hbar\partial_t)\Psi = 0 \tag{2}$$

Do translational transformation to it, we have

$$T_{\vec{\xi}}(t)(h(t) - i\partial_t)T_{\vec{\xi}}^{\dagger}(t)T_{\vec{\xi}}\Psi = \left[T_{\vec{\xi}}(t)(h(t) - i\partial_t)T_{\vec{\xi}}^{\dagger}(t) - i\hbar\partial_t \right] T_{\vec{\xi}}\Psi = 0 \tag{3}$$

where

$$T_{\vec{\xi}} = e^{-\frac{i}{\hbar}\vec{\xi}\cdot\vec{p}}, \ \vec{\xi}(t) = \frac{f_1}{2k_1}\cos(\omega_1 t)\hat{r}_1 + \frac{f_2}{2k_2}\cos(\omega_2 t + \alpha)\hat{r}_2$$

Thus in co-moving frame of reference, Hamiltonian reads

$$
\begin{aligned}
H(t) &= T_{\vec{\xi}}(t)(h(t) - i\partial_t)T_{\vec{\xi}}^{\dagger}(t) \\
&= \frac{p^2}{2\mu} - V_1\cos(2\vec{k_1}\cdot\vec{r_1}) - V_2\cos(2\vec{k_2}\cdot\vec{r_2}) + \dot{\vec{\xi}}(t)\cdot\vec{p} \\
&= \frac{p^2}{2\mu} - V_1\cos(2\vec{k_1}\cdot\vec{r_1}) - V_2\cos(2\vec{k_2}\cdot\vec{r_2}) \\
&\quad + \left[-\left(\frac{\omega_1 f_1}{2k_1}\sin(\omega_1 t) + \frac{\omega_2 f_2}{2k_2}\sin(\omega_2 t + \alpha)\cos(30^\circ)\right)p_x + \frac{\omega_2 f_2}{2k_2}\sin(\omega_2 t + \alpha)\sin(30^\circ)p_y \right] \\
&= \frac{p^2}{2\mu} - V_1\cos(2\vec{k_1}\cdot\vec{r_1}) - V_2\cos(2\vec{k_2}\cdot\vec{r_2}) \\
&\quad + i\frac{\hbar\omega f}{2k_0}\left[\left(\sin(\omega t) + \sin(\omega t + \alpha)\cos(30^\circ)\right)\partial_x - \sin(\omega t + \alpha)\sin(30^\circ)\partial_y\right]
\end{aligned}
$$

Writing Hamiltonian in the form of

$$
H(t) = \sum_n H_n e^{in\omega t} \tag{4}
$$

we obtain

$$
\begin{aligned}
H(t) &= \frac{p^2}{2\mu} - V_1\cos(2\vec{k_1}\cdot\vec{r_1}) - V_2\cos(2\vec{k_2}\cdot\vec{r_2}) \\
&\quad + i\frac{\hbar\omega f}{2k_0}\left[\left(\sin(\omega t) + \sin(\omega t + \alpha)\cos(30^\circ)\right)\partial_x - \sin(\omega t + \alpha)\sin(30^\circ)\partial_y\right] \\
&= \frac{p^2}{2m} - V_1\cos(2\vec{k_1}\cdot\vec{r_1}) - V_2\cos(2\vec{k_2}\cdot\vec{r_2}) \\
&\quad + \frac{\hbar\omega f}{4k_0}\left[\left(1 + \cos(30^\circ)e^{i\alpha}\right)\partial_x - \sin(30^\circ)e^{i\alpha}\partial_y\right]\cdot e^{i\omega t} \\
&\quad - \frac{\hbar\omega f}{4k_0}\left[\left(1 + \cos(30^\circ)e^{-i\alpha}\right)\partial_x - \sin(30^\circ)e^{-i\alpha}\partial_y\right]\cdot e^{-i\omega t} \\
&= H_0 + H_1 e^{i\omega t} + H_{-1} e^{-i\omega t}
\end{aligned} \tag{5}
$$

with

$$
H_0 = \frac{p^2}{2\mu} - V_1\cos(2\vec{k_1}\cdot\vec{r_1}) - V_2\cos(2\vec{k_2}\cdot\vec{r_2}) \tag{6}
$$

$$
H_1 = \frac{\hbar\omega f}{4k_0}\left[\left(1 + \cos(30^\circ)e^{i\alpha}\right)\partial_x - \sin(30^\circ)e^{i\alpha}\partial_y\right] \tag{7}
$$

$$
H_{-1} = H_1^{\dagger} = -\frac{\hbar\omega f}{4k_0}\left[\left(1 + \cos(30^\circ)e^{-i\alpha}\right)\partial_x - \sin(30^\circ)e^{-i\alpha}\partial_y\right] \tag{8}
$$

II C .   Floquet Theory and Effective Hamiltonian

Generally, it might be quite complicated to study the evolution of a system governed by a time-dependent Hamiltonian $H(t)$. However, for a system where the Hamiltonian depends periodically

on time, i.e. $H(t+T) = H(t)$ for some driving period T, Floquet theory provides a powerful frame work for analysis [21–23]. Floquet operator for a periodic time-dependent Hamiltonian is defined as

$$\hat{F} = \hat{U}(T_i + T, T_i) = \hat{T} = \hat{\mathcal{T}} \exp\left(-\mathfrak{i} \int_{T_i}^{T_i+T} \hat{H}(t)\mathrm{d}t \right)$$

where $\hat{\mathcal{T}}$ denotes time order, and T_i is the initial time.

The eigen equation of Floquet operator $\hat{F}$ gives

$$\hat{F}|\varphi_n\rangle = e^{-\mathfrak{i}\varepsilon_n T}|\varphi_n\rangle$$

with eigenvalue $-\pi/T < \varepsilon_n < \pi/T$ and $|\varphi_n\rangle$ the corresponding eigenstate for the n$^{\text{th}}$ quasi-energy band. With the quasi-energy bands spectrum of the Floquet operator, topological properties could be characterized by some topological invariants like winding numbers.

Beside numerically evaluating the Floquet operator directly, one efficient method is to introduce an time-independent Effective Hamiltonian H_{eff} via

$$\hat{F} = e^{-\mathfrak{i}H_{\text{eff}}T}$$

Expanding $\hat{H}(t)$ as

$$\hat{H}(t) = \sum_{n=-\infty}^{\infty} \hat{H}_n(t)e^{i\omega t}$$

H_{eff} can be deduced as[2]

$$\hat{H}_{\text{eff}} = \hat{H}_0 + \sum_{n=1}^{\infty} \left(\frac{[\hat{H}_n, \hat{H}_{-n}]}{n\omega} - \frac{[\hat{H}_n, \hat{H}_0]}{e^{-2\pi ni\alpha}n\omega} + \frac{[\hat{H}_{-n}, \hat{H}_0]}{e^{2\pi ni\alpha}n\omega} \right)$$

---

[2]For details see Appendix A.

III. STATIC LATTICE SOLVING

The Hamiltonian of static two-dimensional triangle optical lattice with intersection angle of $30°$ is

$$H = \frac{p^2}{2\mu} + V(\vec{r})$$

$$V(\vec{r}) = V_1 \cos(2\vec{k_1} \cdot \vec{r_1}) + V_2 \cos(2\vec{k_2} \cdot \vec{r_2})$$

Structure of this lattice in real space is shown in Figure 2a. To help studying the physics in quasi-momentum space, we plot the First Brillioun-Zone of the reciprocal lattice also, which is shown in Figure 2b. In Sec. IV A we will construct tight bounding approximation model of this optical lattice, where we evaluate hopping terms between the Nearest Neighbour sites in the lattice. To see it straightforward, hopping sketch around one specific site has been plotted in Figure 3.

(a) Lattice structure of two-dimensional triangle optical lattice with $30°$ intersection angle in real space

(b) First Brillouin Zone of the Lattice
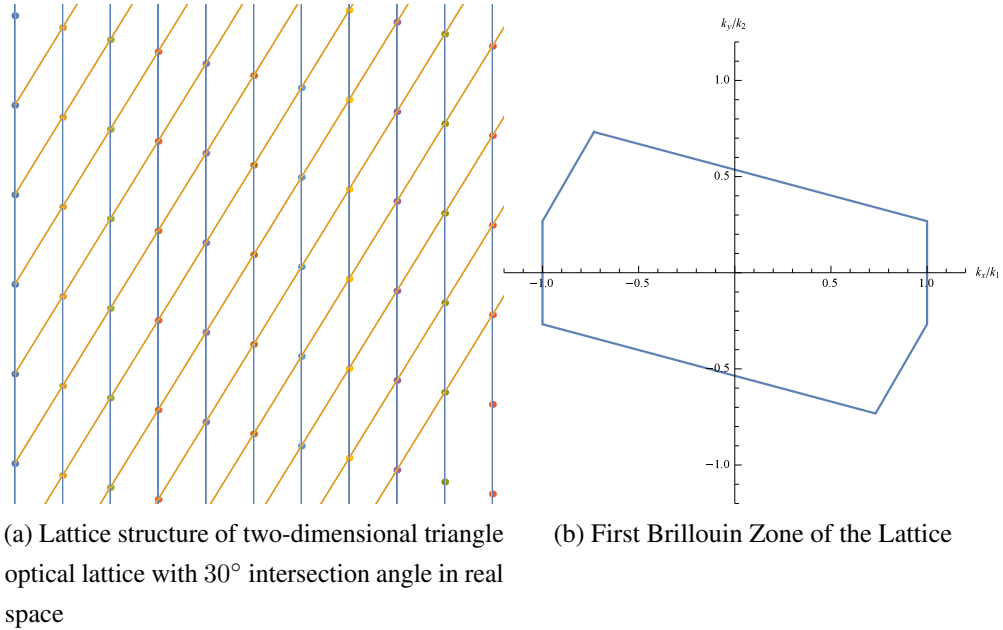
Figure 2: Lattice Structure

The general way to solving such a lattice for energy bands and wave functions is to solving the time-independent Schrödinger equation $H|\psi\rangle = \varepsilon|\psi\rangle$ in a Bloch bases. This is an eigen-problem which could be numerically solved by cutting the Hamiltonian to the subspace expanded by a set of finite bases, i.e., numerically diagonalizing the cut-off Hamiltonian matrix. Energy bands are then acquired, as well as Bloch wave functions. Thus the Wannier functions, localized wave functions in real space, could be obtained by a Fourier transform of the Bloch Functions with respect to the
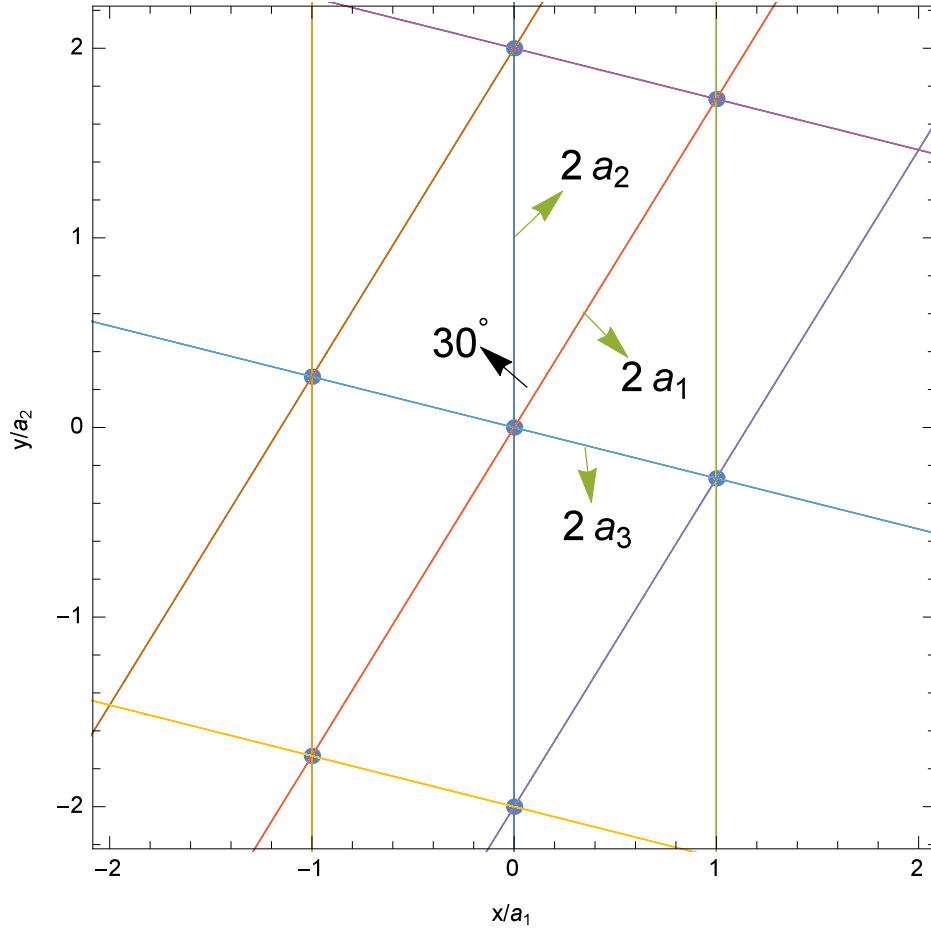
Figure 3: Tight bounding model hopping scheme

Here $2a_1$ and $2a_2$ are the lattice constants we consider to make lattice cell of in real space, with $a_1 = \pi/k_1$, $a_2 = \pi/k_2$. While a_3 is the nearest sites distance in real space in our frame, the value of which could be calculated from a_1, a_2 and the intersection angle, which is, in our model, $30°$. For the simple case that $k_1 = k_2 = k_0$, the lattice constants are $a_1 = a_2 = \pi/k_0$ and $a_3 = (\sqrt{6} - \sqrt{2})\pi/k_0$.

quasi-momentum $\vec{k}$ into real space. After that, Tight-Bounding approximation model could be establish using the results above, which would be studied in Sec. .

III A . Eigen Problem Solving under Bloch Bases

Eigen equation reads

$$H|\psi_q^{(n)}(\vec{r})\rangle = \varepsilon^{(n)}(\vec{k})|\psi_q^{(n)}(\vec{r})\rangle$$

with

$$H = \frac{p^2}{2\mu} + V_1 \cos(2\vec{k_1} \cdot \vec{r_1}) + V_2 \cos(2\vec{k_2} \cdot \vec{r_2})$$

Here superscript n denotes the nth energy band, and $\vec{k}$ refers to the quasi-momentum.

Expand the Bloch wave function with quasi-momentum $\vec{q}$ on the bases of plane wave functions (Bloch bases), we get

$$\psi_q(\vec{r}) = \sum_{l_1,l_2} C_{l_1,l_2}(\vec{q}) e^{i(2l_1\vec{k_1} + 2l_2\vec{k_2} + \vec{q}) \cdot \vec{r}}$$

The matrix elements of Hamiltonian of quasi-momentum $\vec{q}$ under this plane wave bases $\{e^{i(2l_1\vec{k_1}+2l_2\vec{k_2}+\vec{q})\cdot\vec{r}}\}$ could be easily figured out exactly, that

$$
\begin{aligned}
&H_{l_1'l_2',l_1l_2}(\vec{q}) \\
&= \langle l_1'l_2'|H|l_1l_2\rangle \\
&= \left(\frac{1}{2\pi}\right)^2 \int e^{-i(2l_1\vec{k_1}+2l_2\vec{k_2}+\vec{q})\cdot\vec{r}} \left(-\frac{\hbar^2}{2\mu}(\partial_x^2 + \partial_y^2)\right) e^{i(2l_1\vec{k_1}+2l_2\vec{k_2}+\vec{q})\cdot\vec{r}} \mathrm{d}^2r \\
&\quad + \left(\frac{1}{2\pi}\right)^2 \int e^{-i(2l_1\vec{k_1}+2l_2\vec{k_2}+\vec{q})\cdot\vec{r}} \left(V_1 \cos(2\vec{k_1}\cdot\vec{r_1}) + V_2\cos(2\vec{k_2}\cdot\vec{r_2})\right) e^{i(2l_1\vec{k_1}+2l_2\vec{k_2}+\vec{q})\cdot\vec{r}} \mathrm{d}^2r \\
&= \frac{\hbar^2}{2\mu}\left(2l_1\vec{k_1} + 2l_2\vec{k_2} + \vec{q}\right)^2 \left(\frac{1}{2\pi}\right)^2 \int e^{i[(l_1-l_1')2\vec{k_1}+(l_2-l_2')2\vec{k_2}]\cdot\vec{r}}\mathrm{d}^2r \\
&\quad + \frac{1}{2}V_1\left[\left(\frac{1}{2\pi}\right)^2 \int e^{i[(l_1-l_1'-1)2\vec{k_1}+(l_2-l_2')2\vec{k_2}]\cdot\vec{r}}\mathrm{d}^2r + \left(\frac{1}{2\pi}\right)^2 \int e^{i[(l_1-l_1'+1)2\vec{k_1}+(l_2-l_2')2\vec{k_2}]\cdot\vec{r}}\mathrm{d}^2r\right] \\
&\quad + \frac{1}{2}V_2\left[\left(\frac{1}{2\pi}\right)^2 \int e^{i[(l_1-l_1')2\vec{k_1}+(l_2-l_2'-1)2\vec{k_2}]\cdot\vec{r}}\mathrm{d}^2r + \left(\frac{1}{2\pi}\right)^2 \int e^{i[(l_1-l_1')2\vec{k_1}+(l_2-l_2'+1)2\vec{k_2}]\cdot\vec{r}}\mathrm{d}^2r\right] \\
&= \frac{\hbar^2}{2\mu}\left(2l_1\vec{k_1} + 2l_2\vec{k_2} + \vec{q}\right)^2 \delta_{l_1'l_1}\delta_{l_2'l_2} \\
&\quad + \frac{1}{2}V_1(\delta_{l_1,l_1'-1}\delta_{l_2,l_2'} + \delta_{l_1,l_1'+1}\delta_{l_2,l_2'}) + \frac{1}{2}V_2(\delta_{l_1,l_1'}\delta_{l_2,l_2'-1} + \delta_{l_1,l_1'}\delta_{l_2,l_2'+1})
\end{aligned}
$$

With the help of this exact expression of each elements in the (cut-off) Hamiltonian matrix, a numerical method of diagonalization is approached to this cut-off matrix and we obtain the energy bands of this two-dimensional triangle lattice with the corresponding Bloch wave functions.

Some energy bands with different potential depth are plotted in Figure 4 - 7. Here we take $\epsilon_0 = \hbar^2 k_0^2 / 2\mu$ as energy unit. To examine whether the results are reasonable, we calculate the energy bands for a very small potential depth, that $V_1 = V_2 = 0.05\epsilon_0$, approximate to zero. Theoretically, the asymptotic behavior when potential depth close to zero tends to be like a free particle, which means the energy gap tends to disappear that next energy bands getting touched, and the whole energy spectrum is a little bit varied from a quadratic form. Our numerical results show this character as expected, which are plotted in Figure 8 . It shows from Figure 8a that four lowest energy bands of potential depth $V_1 = V_2 = 0.05\epsilon_0$ almost touch together, which is quite distinguished from the large potential depth cases where energy bands are separated by large gaps, referring to Figure 4a ($V_1 = V_2 = 1.0\epsilon_0$), Figure 5a ($V_1 = V_2 = 2.0\epsilon_0$), Figure 6a ($V_1 = V_2 = 8.0\epsilon_0$), and Figure 7a ($V_1 = V_2 = 16.0\epsilon_0$). Besides, Figure 8d is a top view to the lowest energy band, from which we see clearly what the first Brillioun Zone looks like. It shows the the same contour as we have showed in Figure 2b.

(a) The lowest four bands

(b) Band 1

(c) Band 2

(d) Band 3
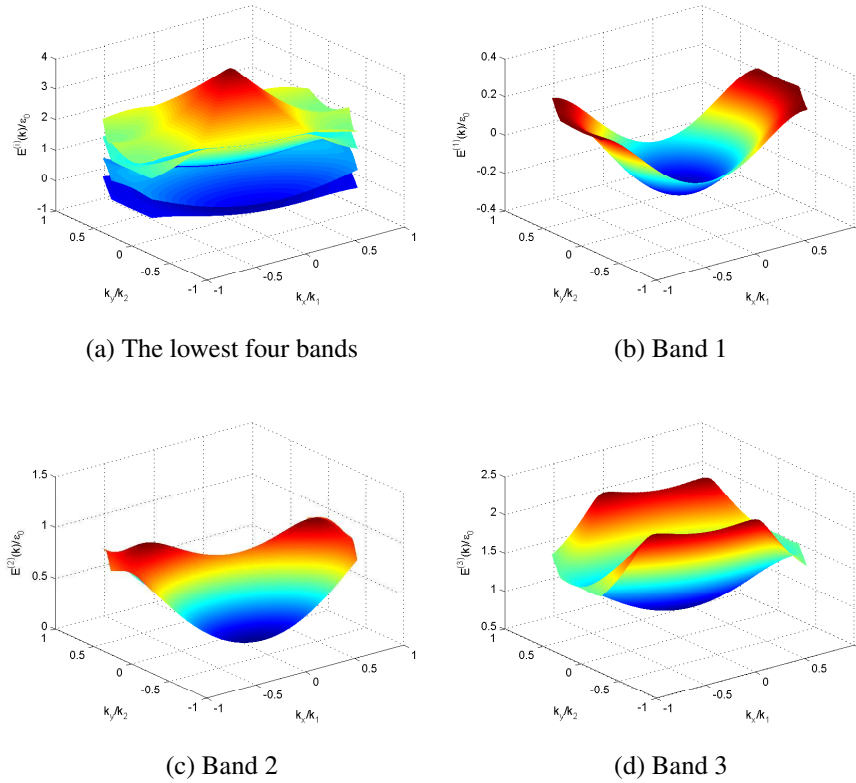
Figure 4: Energy bands plotting within the First Brilllioun Zone. Potential depth $V_1 = V_2 = 1.0$ Taking $\epsilon_0 = \hbar^2 k_0^2 / 2\mu$ as energy unit, similarly hereinafter.

(a) The lowest four bands

(b) Band 1

(c) Band 2

(d) Band 3
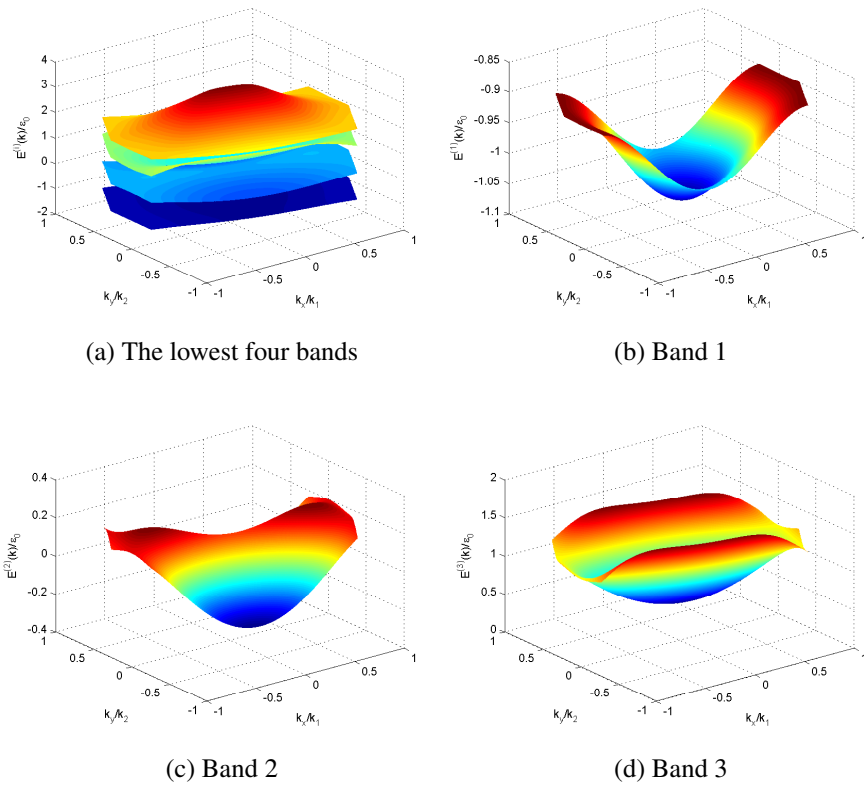
Figure 5: Energy bands with potential depth $V_1 = V_2 = 2.0$

(a) The lowest four bands

(b) Band 1

(c) Band 2

(d) Band 3
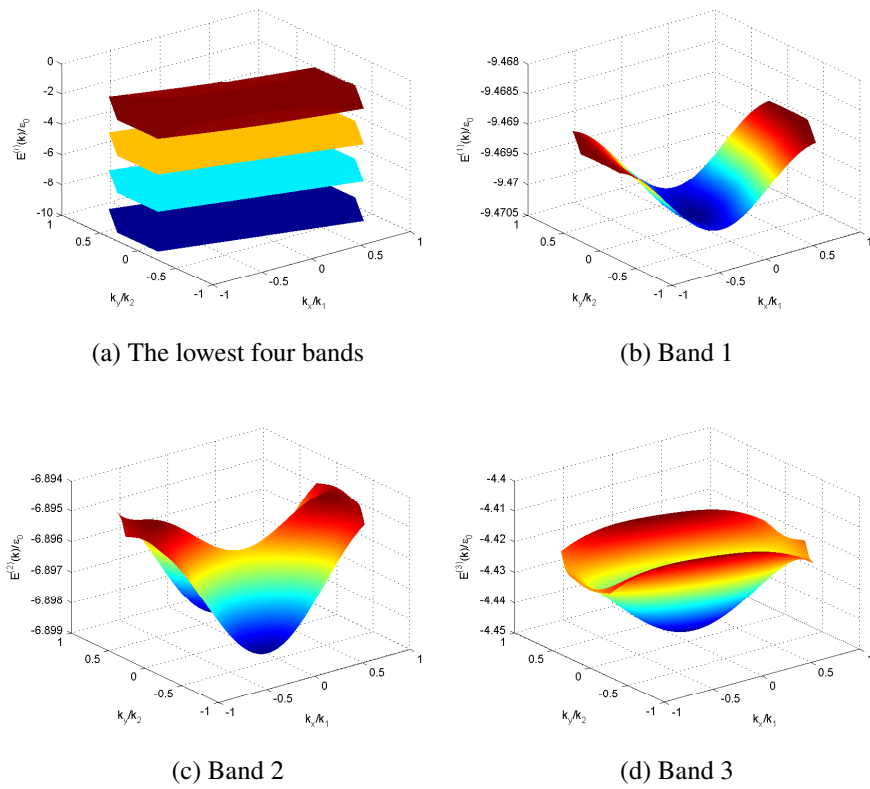
Figure 6: Energy bands with potential depth $V_1 = V_2 = 8.0$

(a) The lowest four bands

(b) Band 1

(c) Band 2

(d) Band 3
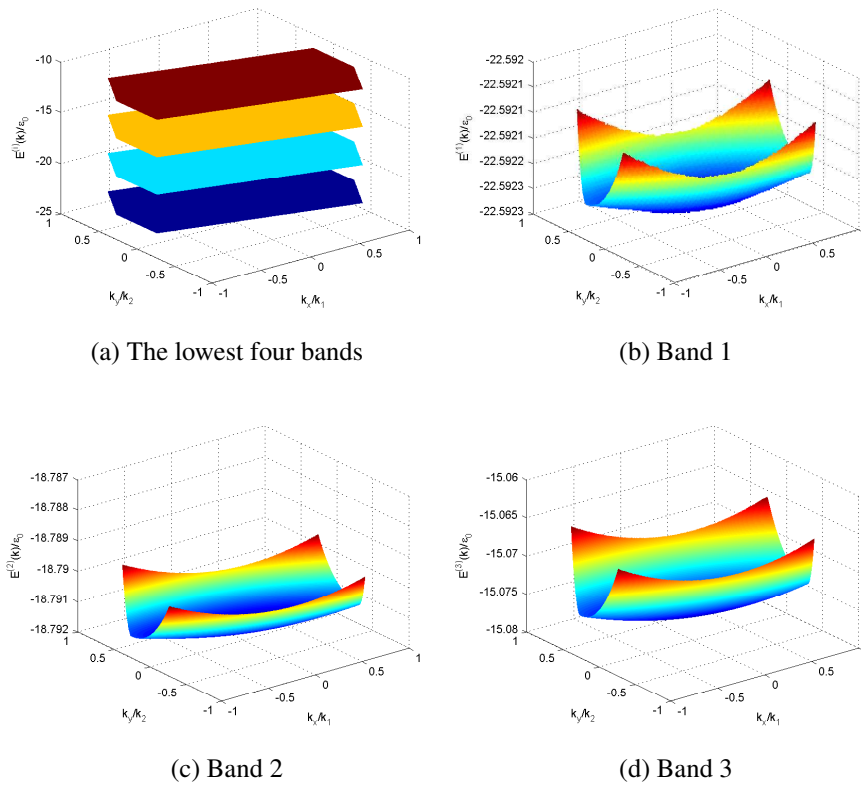
Figure 7: Energy bands with potential depth $V_1 = V_2 = 16.0$

(a) The lowest four bands

(b) Band 1

(c) Band 2

(d) Top View for the lowest band

Figure 8: Energy bands with potential depth $V_1 = V_2 = 0.05$

III B .   Wannier Functions

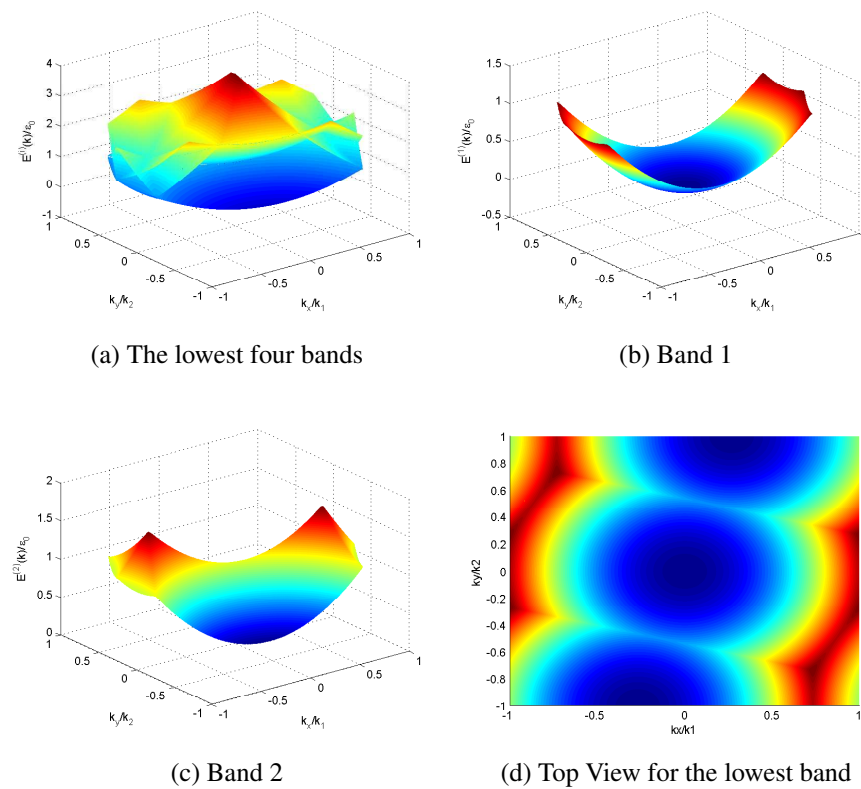Analytically, Wannier functions can be obtained from the Bloch functions by a Fourier transform of the Bloch functions into real space with respect to the quasi-momentum $\vec{k}$.

$$w_n(\vec{R}_m, \vec{r}) = w_n(\vec{r} - \vec{R}_m) = \frac{1}{\sqrt{N}} \sum_{\vec{k} \in BZ} e^{-i\vec{k} \cdot \vec{R}_m} \psi_{n\vec{k}}(\vec{r})$$

Here $\psi_{n\vec{k}}$ is the bloch function with quasi-momentum of $\vec{k}$, and $\vec{R}_m$ refers to the lattice sites.

We numerically approach this method to get Wannier functions localized around the origin of the real space by quantizing the following Eq. 9 and numerically evaluate it.[3]

$$
\begin{aligned}
w_n(\vec{r}) = w_n(0, \vec{r}) &= \frac{1}{\sqrt{N}} \sum_{\vec{q} \in BZ} \psi_{n\vec{q}}(\vec{r}) \\
&= \frac{1}{\sqrt{N}} \sum_{\vec{q} \in BZ} \sum_{l_1, l_2} C_{l_1, l_2}(\vec{q}) e^{i(2l_1\vec{k}_1 + 2l_2\vec{k}_2 + \vec{q}) \cdot \vec{r}}
\end{aligned}
\tag{9}
$$

Here plot some Wannier Functions in Figure 9 . In these figures, we choose the potential depth to be $V_1 = V_2 = 8.0\epsilon_0$, and plotting the Wannier functions of the lowest four bands. The square of modulus of the Wannier functions for the lowest two bands are also plotted in Figure 10.

Figure 9 shows that the Wannier functions are well localized in real space, and tends to disappear with a rapid damped oscillation around zero when going away from the origin.

---

[3]Program code seeing Appendix B − 4

(a) Wannier function for the 1ˢᵗ band $w_1(x, y)$

(b) Wannier function for the 2ⁿᵈ band $w_2(x, y)$

(c) Wannier function for the 3ᵗʰ band $w_3(x, y)$

(d) Wannier function for the 4ᵗʰ band $w_4(x, y)$
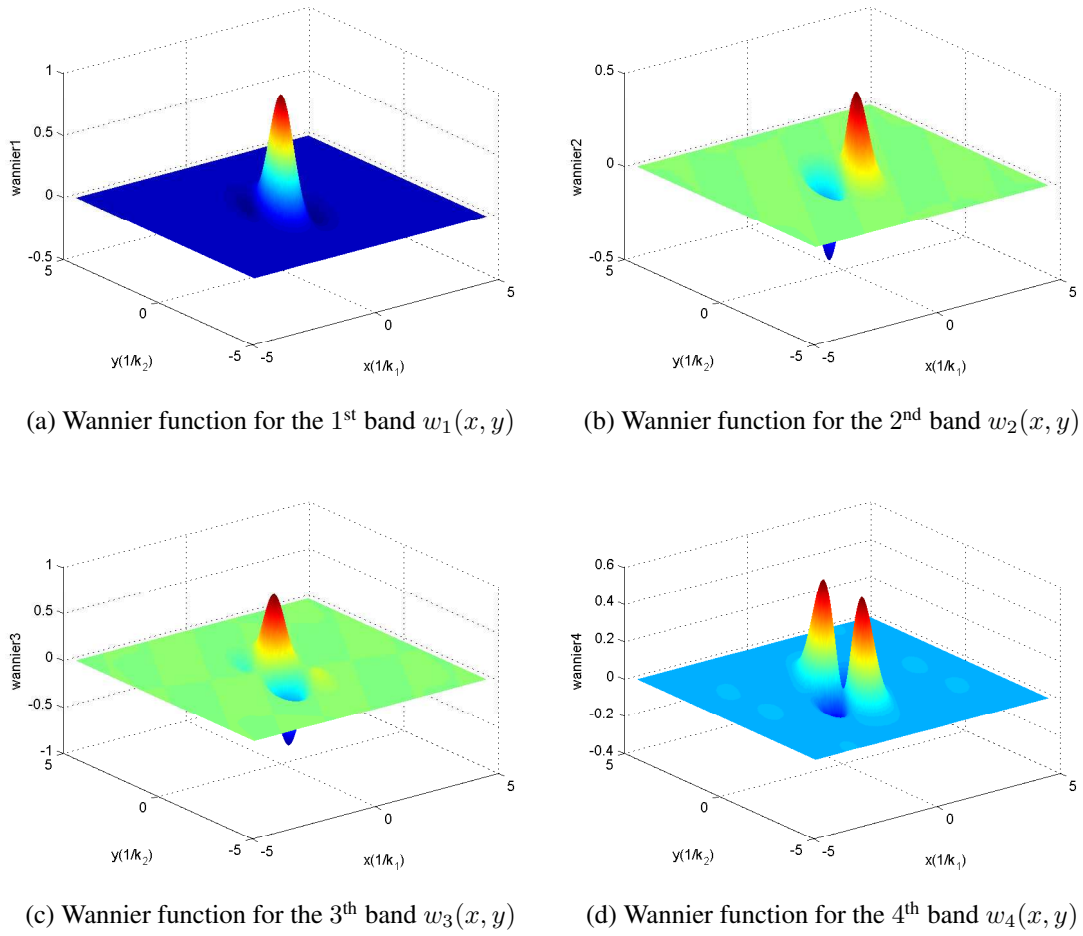
Figure 9: Wannier functions with potential detph $V_1 = V_2 = 8.0$

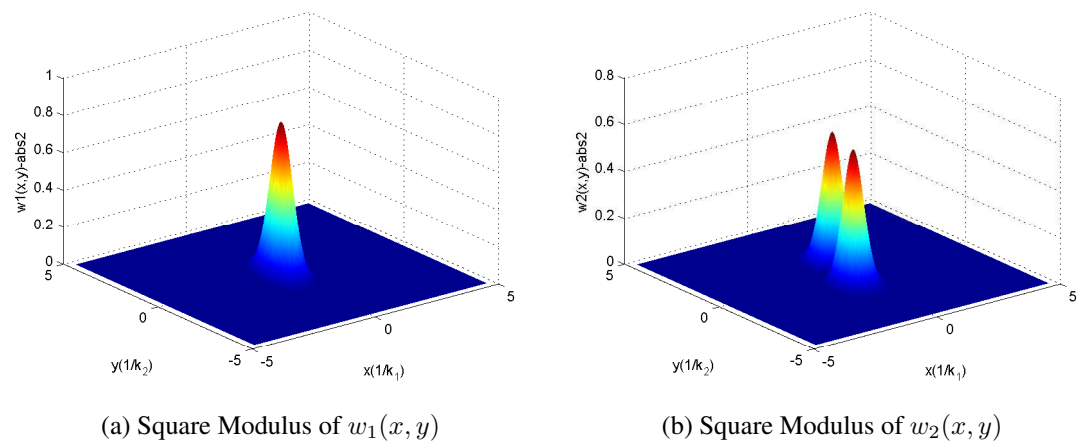(a) Square Modulus of $w_1(x, y)$

(b) Square Modulus of $w_2(x, y)$

Figure 10: Square modulus of the Wannier functions in Figure 9

IV. EFFECTIVE HAMILTONIAN FOR TIGHT BOUNDING APPROXIMATION MODEL

IV A. Tight Bounding Approximation

Second quantized Hamiltonian under Wannier bases reads

$$\hat{H}(t) = \int \mathrm{d}^2 r \hat{\Psi}^\dagger(\vec{r}) H(t) \hat{\Psi}(\vec{r}) = \sum_{\substack{\lambda'\lambda \\ \vec{m}\vec{n}}} H_{\lambda'\lambda}^{(\vec{m},n)}(t) \hat{a}_{\lambda'\vec{m}}^\dagger \hat{a}_{\lambda\vec{n}}$$

with

$$\hat{\Psi}(\vec{r}) = \sum_{\lambda\vec{n}} \hat{a}_{\lambda\vec{n}} w_\lambda(\vec{r} - \vec{R}_n)$$

$$H_{\lambda'\lambda}^{(\vec{m},n)}(t) = \int \mathrm{d}^2 r w_{\lambda'}^*(\vec{r} - \vec{R}_m) H(t) w_\lambda(\vec{r} - \vec{R}_n)$$

and $\hat{a}^\dagger$ and $\hat{a}$ are the creative and annihilative operators. For translational symmetry possessed by the lattice, $H_{\lambda'\lambda}^{(\vec{m},n)}(t) = H_{\lambda'\lambda}^{(\vec{m}-\vec{n})}(t)$ depends only on $\vec{m} - \vec{n}$.

Take Fourier transform with respect to $\vec{r}$,

$$\hat{a}_{\lambda'\vec{m}}^\dagger = \frac{1}{\sqrt{L}} \sum_{\vec{k}} e^{-i\vec{k}\cdot\vec{R}_m} \hat{a}_{\lambda'\vec{k}}^\dagger, \quad \hat{a}_{\lambda\vec{n}} = \frac{1}{\sqrt{L}} \sum_{\vec{k}} e^{i\vec{k}\cdot\vec{R}_n} \hat{a}_{\lambda\vec{k}}$$

Thus Hamiltonian in the quasi-momentum space, with $\vec{\delta} = \vec{R}_m - \vec{R}_n$, writes

$$\hat{H}(t) = \sum_{\vec{k}} \hat{H}_{\lambda'\lambda}(\vec{k}), \quad \hat{H}_{\lambda'\lambda}(\vec{k}) = \sum_{\lambda'\lambda,\vec{\delta}} e^{i\vec{k}\cdot\vec{\delta}} H_{\lambda'\lambda}^{\vec{\delta}}(t) \hat{a}_{\lambda'\vec{k}}^\dagger \hat{a}_{\lambda\vec{k}}$$

Cutting off the Hamiltonian within the subspace expanded by the lowest two bands (denoted as s band and p band), it becomes

$$\hat{H}(t) = \sum_{\vec{k}} \begin{pmatrix} \hat{a}_{s\vec{k}}^\dagger & \hat{a}_{p\vec{k}}^\dagger \end{pmatrix} H(\vec{k}, t) \begin{pmatrix} \hat{a}_{s\vec{k}} \\ \hat{a}_{p\vec{k}} \end{pmatrix}$$

and

$$H(\vec{k}, t) = H_0(\vec{k}) + H_1(\vec{k}) e^{i\omega t} + H_{-1}(\vec{k}) e^{-i\omega t}$$

Tight bounding approximation considers merely the nearest sites hopping. So $\vec{\delta} = \vec{R}_m - \vec{R}_n = 0, or \vec{\gamma_i}$, where $\vec{\gamma_i}$ is the crystal lattice vectors or nearest sites vectors. Thus we could write $H(\vec{k})$ as

$$H_0(\vec{k}) = \begin{bmatrix} H_{11}^{(0)} & H_{12}^{(0)} \\ H_{21}^{(0)} & H_{22}^{(0)} \end{bmatrix} \quad H_1(\vec{k}) = \begin{bmatrix} H_{11}^{(1)} & H_{12}^{(1)} \\ H_{21}^{(1)} & H_{22}^{(1)} \end{bmatrix} \quad H_{-1}(\vec{k}) = \begin{bmatrix} H_{11}^{(-1)} & H_{12}^{(-1)} \\ H_{21}^{(-1)} & H_{22}^{(-1)} \end{bmatrix}$$

where

$$H_{\lambda'\lambda}^{(i)} = \langle w_{\lambda'}(\vec{r})|H_i|w_\lambda(\vec{r})\rangle + \sum_{n.n} e^{i\vec{k}\cdot\vec{R_m}} \langle w_{\lambda'}(\vec{r} - \vec{R_m})|H_i|w_\lambda(\vec{r})\rangle$$

Here n.n means that summation includes only the nearest sites.

Thus we obtain

$$H_0(\vec{k}) = \begin{bmatrix} E_s & iK \\ -iK & E_p \end{bmatrix} \quad H_1(\vec{k}) = \begin{bmatrix} \Lambda_s & \Omega \\ -\Omega & \Lambda_p \end{bmatrix} \quad H_{-1}(\vec{k}) = H_1(\vec{k})^\dagger = \begin{bmatrix} \Lambda_s^* & -\Omega^* \\ \Omega^* & \Lambda_p^* \end{bmatrix}$$

with

$$
\begin{aligned}
E_s &= \epsilon_s + 2\Big[t_s^{(1)}\cos(2\vec{k}\cdot\vec{a_1}) + t_s^{(2)}\cos(2\vec{k}\cdot\vec{a_2}) + t_s^{(3)}\cos(2\vec{k}\cdot\vec{a_3})\Big] \\
E_p &= \epsilon_p + 2\Big[t_p^{(1)}\cos(2\vec{k}\cdot\vec{a_1}) + t_p^{(2)}\cos(2\vec{k}\cdot\vec{a_2}) + t_p^{(3)}\cos(2\vec{k}\cdot\vec{a_3})\Big] \\
K &= 2\Big[t_{sp}^{(1)}\sin(2\vec{k}\cdot\vec{a_1}) + t_{sp}^{(2)}\sin(2\vec{k}\cdot\vec{a_2}) + t_{sp}^{(3)}\sin(2\vec{k}\cdot\vec{a_3})\Big] \\
\Lambda_s &= i2\Big[h_s^{(1)}\sin(2\vec{k}\cdot\vec{a_1}) + h_s^{(2)}\sin(2\vec{k}\cdot\vec{a_2}) + h_s^{(3)}\sin(2\vec{k}\cdot\vec{a_3})\Big] \\
\Lambda_p &= i2\Big[h_p^{(1)}\sin(2\vec{k}\cdot\vec{a_1}) + h_p^{(2)}\sin(2\vec{k}\cdot\vec{a_2}) + h_p^{(3)}\sin(2\vec{k}\cdot\vec{a_3})\Big] \\
\Omega &= h_{sp}^{(0)} + 2\Big[h_{sp}^{(1)}\cos(2\vec{k}\cdot\vec{a_1}) + h_{sp}^{(2)}\cos(2\vec{k}\cdot\vec{a_2}) + h_{sp}^{(3)}\cos(2\vec{k}\cdot\vec{a_3})\Big]
\end{aligned}
\tag{10}
$$

or in a more compact form,

$$
\begin{aligned}
E_s &= \epsilon_s + 2\sum_{j=1}^{3} t_s^{(j)}\cos(2\vec{k}\cdot\vec{a_j}) \\
E_p &= \epsilon_p + 2\sum_{j=1}^{3} t_p^{(j)}\cos(2\vec{k}\cdot\vec{a_j}) \\
K &= 2\sum_{j=1}^{3} t_{sp}^{(j)}\sin(2\vec{k}\cdot\vec{a_j}) \\
\Lambda_s &= i2\sum_{j=1}^{3} h_s^{(j)}\sin(2\vec{k}\cdot\vec{a_j}) \\
\Lambda_p &= i2\sum_{j=1}^{3} h_p^{(j)}\sin(2\vec{k}\cdot\vec{a_j}) \\
\Omega &= h_{sp}^{(0)} + 2\sum_{j=1}^{3} h_{sp}^{(j)}\cos(2\vec{k}\cdot\vec{a_j})
\end{aligned}
\tag{11}
$$

Here the hopping integral are, exactly, as follow:

$$\epsilon_s = \langle s|H_0|s\rangle = -\frac{\hbar^2}{2\mu}\langle s|\partial_x^2 + \partial_y^2|s\rangle + \langle s|V(\vec{r})|s\rangle$$

$$\epsilon_p = \langle p|H_0|p\rangle = -\frac{\hbar^2}{2\mu}\langle p|\partial_x^2 + \partial_y^2|p\rangle + \langle p|V(\vec{r})|p\rangle$$

$$t_s^{(j)} = \langle s(j)|H_0|s\rangle = -\frac{\hbar^2}{2\mu}\langle s(i)|\partial_x^2 + \partial_y^2|s\rangle + \langle s|V(\vec{r})|s\rangle$$

$$t_p^{j)} = \langle p(j)|H_0|p\rangle = -\frac{\hbar^2}{2\mu}\langle p(i)|\partial_x^2 + \partial_y^2|p\rangle + \langle p(i)|V(\vec{r})|p\rangle$$

$$t_{sp}^{(j)} = \langle s(j)|H_0|p\rangle = -\frac{\hbar^2}{2\mu}\langle s(i)|\partial_x^2 + \partial_y^2|p\rangle + \langle s(i)|V(\vec{r})|p\rangle \tag{12}$$

$$h_s^{(j)} = \langle s(j)|H_1|s\rangle = \frac{\hbar\omega f}{4k_0}\Big[(1 + \cos(30°)e^{i\alpha})\langle s(i)|\partial_x|s\rangle + \sin(-30°)e^{i\alpha}\langle s(i)|\partial_y|s\rangle\Big]$$

$$h_p^{(j)} = \langle p(j)|H_1|p\rangle = \frac{\hbar\omega f}{4k_0}\Big[(1 + \cos(30°)e^{i\alpha})\langle p(i)|\partial_x|p\rangle + \sin(-30°)e^{i\alpha}\langle p(i)|\partial_y|p\rangle\Big]$$

$$h_{sp}^{(j)} = \langle s(j)|H_1|p\rangle = \frac{\hbar\omega f}{4k_0}\Big[(1 + \cos(30°)e^{i\alpha})\langle s(i)|\partial_x|p\rangle + \sin(-30°)e^{i\alpha}\langle s(i)|\partial_y|p\rangle\Big]$$

Or, in a more compact way,

$$t_{\lambda'\lambda}^{(j)} = \langle \lambda'(j)|H_0|\lambda\rangle = -\frac{\hbar^2}{2\mu}\langle \lambda'(j)|\partial_x^2 + \partial_y^2|\lambda\rangle + \langle \lambda'(j)|V(\vec{r})|\lambda\rangle$$

$$h_{\lambda'\lambda}^{(j)} = \langle \lambda'(j)|H_1|\lambda\rangle = \frac{\hbar\omega f}{4k_0}\Big[(1 + \cos(30°)e^{i\alpha})\langle \lambda'(j)|\partial_x|\lambda\rangle + \sin(-30°)e^{i\alpha}\langle \lambda'(j)|\partial_y|\lambda\rangle\Big] \tag{13}$$

$$\epsilon_s = t_s^{(0)}, \quad \epsilon_p = t_p^{(0)}$$

From above we see, t is real, while h is complex. And t is related to the potential depth V_1, V_2, while h is related to the shaking frequency ω and shaking amplitude f. Denoting $\bar{f} = f/k_0$, $\bar{\omega} = \hbar\omega$, and expressing the h terms in a form that real parts is separated with the imaginary parts, we can rewrite the h terms as follows.

$$h_{\lambda'\lambda}^{(j)} = \frac{1}{4}\bar{f}\bar{\omega}\big[(r_{\lambda'\lambda}^{(j)} + \cos\alpha \cdot u_{\lambda'\lambda}^{(j)}) + i\sin\alpha \cdot u_{\lambda'\lambda}^{(j)}\big]$$

where

$$r_{\lambda'\lambda}^{(j)} = \langle \lambda'(j)|\partial_x|\lambda\rangle$$

$$u_{\lambda'\lambda}^{(j)} = \cos 30°\langle \lambda'(j)|\partial_x|\lambda\rangle + \sin(-30°)\langle \lambda'(j)|\partial_y|\lambda\rangle$$

Thus for a given potential, $r_{\lambda'\lambda}^{(j)}$, $s_{\lambda'\lambda}^{(j)}$ possess fixed real value, while $\Lambda_s(\vec{k})$, $\Lambda_p(\vec{k})$ and $\Omega(\vec{k})$

are proportional to $\bar{f}$ and $\bar{\omega}$. That we have

$$\Lambda_s = \mathfrak{i}2\sum_{j=1}^{3} h_s^{(j)} \sin(2\vec{k}\cdot\vec{a_j})$$

$$= \frac{1}{2}\bar{f}\bar{\omega}\sum_{j=1}^{3}\Big[-\sin\alpha\cdot u_s^{(j)} + \mathfrak{i}(r_s^{(j)}+\cos\alpha\cdot u_s^{(j)})\Big]\sin(2\vec{k}\cdot\vec{a_j})$$

$$\Lambda_p = \mathfrak{i}2\sum_{j=1}^{3} h_p^{(j)} \sin(2\vec{k}\cdot\vec{a_j})$$

$$= \frac{1}{2}\bar{f}\bar{\omega}\sum_{j=1}^{3}\Big[-\sin\alpha\cdot u_p^{(j)} + \mathfrak{i}(r_p^{(j)}+\cos\alpha\cdot u_p^{(j)})\Big]\sin(2\vec{k}\cdot\vec{a_j}) \tag{14}$$

$$\Omega = h_{sp}^{(0)} + 2\sum_{j=1}^{3} h_{sp}^{(j)} \cos(2\vec{k}\cdot\vec{a_j})$$

$$= \frac{1}{4}\bar{f}\bar{\omega}\Bigg[r_{sp}^{(0)} + \cos\alpha u_{sp}^{(0)} - 2\sin\alpha\sum_{j=1}^{3} u_{sp}^{(j)}\cos(2\vec{k}\cdot\vec{a_j})$$

$$+ \mathfrak{i}\Big(\sin\alpha u_{sp}^{(0)} + 2\sum_{j=1}^{3}\big(r_{sp}^{(j)}+\cos\alpha u_{sp}^{(j)}\big)\cos(2\vec{k}\cdot\vec{a_j})\Big)\Bigg]$$

and

$$\Re(\Lambda_s) = -\frac{1}{2}\bar{f}\bar{\omega}\sum_{j=1}^{3}\sin\alpha u_s^{(j)}\sin(2\vec{k}\cdot\vec{a_j}) \tag{15a}$$

$$\Im(\Lambda_s) = \frac{1}{2}\bar{f}\bar{\omega}\sum_{j=1}^{3}\big(r_s^{(j)}+\cos\alpha u_s^{(j)}\big)\sin(2\vec{k}\cdot\vec{a_j}) \tag{15b}$$

$$\Re(\Lambda_p) = -\frac{1}{2}\bar{f}\bar{\omega}\sum_{j=1}^{3}\sin\alpha u_p^{(j)}\sin(2\vec{k}\cdot\vec{a_j}) \tag{16a}$$

$$\Im(\Lambda_p) = \frac{1}{2}\bar{f}\bar{\omega}\sum_{j=1}^{3}\big(r_p^{(j)}+\cos\alpha u_p^{(j)}\big)\sin(2\vec{k}\cdot\vec{a_j}) \tag{16b}$$

$$\Re(\Omega) = \frac{1}{4}\bar{f}\bar{\omega}\Big(r_{sp}^{(0)} + \cos\alpha u_{sp}^{(0)} - 2\sin\alpha\sum_{j=1}^{3} u_{sp}^{(j)}\cos(2\vec{k}\cdot\vec{a_j})\Big) \tag{17a}$$

$$\Im(\Omega) = \frac{1}{4}\bar{f}\bar{\omega}\Big(\sin\alpha u_{sp}^{(0)} + 2\sum_{j=1}^{3}\big(r_{sp}^{(j)}+\cos\alpha u_{sp}^{(j)}\big)\cos(2\vec{k}\cdot\vec{a_j})\Big) \tag{17b}$$

Here $\Re$ and $\Im$ means the real part and imaginary part of the complex number, respectively.

IV B. Effective Hamiltonian

For one-phonon resonance condition, do a unitary transformation to the Hamiltonian, that

$$\widetilde{H}(\vec{k},t) = U(t)(H(\vec{k},t) - i\partial_t)U^\dagger(t) = \sum_n \widetilde{H}_n e^{in\omega t} = \widetilde{H}_0 + \sum_{n=\pm1\pm2} \widetilde{H}_n e^{in\omega t}$$

with

$$U(t) = \begin{bmatrix} e^{-i\omega t} & 0 \\ 0 & 1 \end{bmatrix}$$

and

$$\widetilde{H}_0(\vec{k}) = \begin{bmatrix} E_s + \omega & \Omega \\ \Omega^* & E_p \end{bmatrix}$$

$$\widetilde{H}_1(\vec{k}) = \begin{bmatrix} \Lambda_s & 0 \\ -iK & \Lambda_p \end{bmatrix} \qquad \widetilde{H}_{-1}(\vec{k}) = \begin{bmatrix} \Lambda_s^* & iK \\ 0 & \Lambda_p^* \end{bmatrix} = H_1^\dagger$$

$$\widetilde{H}_2(\vec{k}) = \begin{bmatrix} 0 & 0 \\ -\Omega & 0 \end{bmatrix} \qquad \widetilde{H}_{-2}(\vec{k}) = \begin{bmatrix} 0 & -\Omega^* \\ 0 & 0 \end{bmatrix} = H_2^\dagger$$

$$\hat{H}_{\text{eff}} = \hat{H}_0 + \sum_{n=1}^\infty \left(\frac{[\hat{H}_n, \hat{H}_{-n}]}{n\omega} - \frac{[\hat{H}_n, \hat{H}_0]}{e^{-2\pi ni\alpha}n\omega} + \frac{[\hat{H}_{-n}, \hat{H}_0]}{e^{2\pi ni\alpha}n\omega} \right)$$

$$\widetilde{H}_0(\vec{k}) = \begin{bmatrix} E_s + \omega & \Omega \\ \Omega^* & E_p \end{bmatrix} = \frac{E_s + \omega + E_p}{2} + \frac{E_s + \omega - E_p}{2}\sigma_z + \Omega\sigma_+ + \Omega^*\sigma_-$$

$$\widetilde{H}_1(\vec{k}) = \begin{bmatrix} \Lambda_s & 0 \\ -iK & \Lambda_p \end{bmatrix} = \frac{\Lambda_s + \Lambda_p}{2} + \frac{\Lambda_s - \Lambda_p}{2}\sigma_z - iK\sigma_-$$

$$\widetilde{H}_{-1}(\vec{k}) = \begin{bmatrix} \Lambda_s^* & iK \\ 0 & \Lambda_p^* \end{bmatrix} = \frac{\Lambda_s^* + \Lambda_p^*}{2} + \frac{\Lambda_s^* - \Lambda_p^*}{2}\sigma_z + iK\sigma_+$$

$$\widetilde{H}_2(\vec{k}) = \begin{bmatrix} 0 & 0 \\ -\Omega & 0 \end{bmatrix} = -\Omega\sigma_-$$

$$\widetilde{H}_{-2}(\vec{k}) = \begin{bmatrix} 0 & -\Omega^* \\ 0 & 0 \end{bmatrix} = -\Omega^*\sigma_+$$

Here σ are the pauli matrices,

$$\sigma_z = \begin{bmatrix} 1 & 0 \\ 0 & -1 \end{bmatrix} \quad \sigma_x = \begin{bmatrix} 0 & 1 \\ 1 & 0 \end{bmatrix} \quad \sigma_y = \begin{bmatrix} 0 & -i \\ i & 0 \end{bmatrix}$$

$$\sigma_+ = \begin{bmatrix} 0 & 1 \\ 0 & 0 \end{bmatrix} \quad \sigma_- = \begin{bmatrix} 0 & 0 \\ 1 & 0 \end{bmatrix}$$

$$or\,, \quad \sigma_\pm = \frac{1}{2}(\sigma_x \pm i\sigma_y)$$

Therefore

$$[\widetilde{H}_1(\vec{k}), \widetilde{H}_{-1}(\vec{k})] = \begin{bmatrix} -K^2 & +iK(\Lambda_s - \Lambda_p) \\ iK(\Lambda_s^* - \Lambda_p^*) & K^2 \end{bmatrix} = -K^2\sigma_z + iK(\Lambda_s - \Lambda_p)\sigma_+ - iK(\Lambda_s^* - \Lambda_p^*)\sigma_-$$

$$[\widetilde{H}_2(\vec{k}), \widetilde{H}_{-2}(\vec{k})] = \begin{bmatrix} -|\Omega|^2 & 0 \\ 0 & |\Omega|^2 \end{bmatrix} = -|\Omega|^2\sigma_z$$

And

$$\begin{aligned}
\widetilde{H}_{\text{eff}}(\vec{k}) &= \widetilde{H}_0(\vec{k}) + \frac{1}{\omega}[\widetilde{H}_1(\vec{k}), \widetilde{H}_{-1}(\vec{k})] + \frac{1}{2\omega}[\widetilde{H}_2(\vec{k}), \widetilde{H}_{-2}(\vec{k})] \\
&= \frac{1}{2}(E_s + \omega + E_p) + \frac{1}{2}(E_s + \omega - E_p)\sigma_z + \Omega\sigma_+ + \Omega^*\sigma_- \\
&\quad + \frac{1}{\omega}\Big(-K^2\sigma_z + iK(\Lambda_s - \Lambda_p)\sigma_+ - iK(\Lambda_s^* - \Lambda_p^*)\sigma_-\Big) - \frac{|\Omega|^2}{2\omega}\sigma_z \\
&= \frac{1}{2}(E_s + \omega + E_p) + \Big(\frac{E_s + \omega - E_p}{2} - \frac{K^2}{\omega} - \frac{|\Omega|^2}{2\omega}\Big)\sigma_z \\
&\quad + \Big(\Omega + i\frac{K}{\omega}(\Lambda_s - \Lambda_p)\Big)\sigma_+ + \Big(\Omega^* - i\frac{K}{\omega}(\Lambda_s^* - \Lambda_p^*)\Big)\sigma_- \\
&= \frac{1}{2}(E_s + \omega + E_p) \\
&\quad + \Big(\frac{E_s + \omega - E_p}{2} - \frac{K^2}{\omega} - \frac{|\Omega|^2}{2\omega}\Big)\sigma_z \\
&\quad + \Big(\Re(\Omega) - \frac{K}{\omega}(\Im(\Lambda_s) - \Im(\Lambda_p))\Big)\sigma_x \\
&\quad + \Big(-\Im(\Omega) - \frac{K}{\omega}(\Re(\Lambda_s) - \Re(\Lambda_p))\Big)\sigma_y
\end{aligned}$$

Thus the effective Hamiltonian can be written as

$$\begin{aligned}
\widetilde{H}_{\text{eff}}(\vec{k}) &= \varepsilon_0 + \vec{B}(\vec{k}) \cdot \vec{\sigma} \\
&= \varepsilon_0 + B_x(\vec{k})\sigma_x + B_y(\vec{k})\sigma_y + B_z(\vec{k})\sigma_z
\end{aligned}$$

with

$$\varepsilon_0 = \frac{1}{2}(E_s + \omega + E_p)$$

$$B_x(\vec{k}) = \Re(\Omega) + \frac{K}{\omega}\big(\Im(\Lambda_p) - \Im(\Lambda_s)\big)$$

$$B_y(\vec{k}) = -\Im(\Omega) + \frac{K}{\omega}\big(\Re(\Lambda_p) - \Re(\Lambda_s)\big)$$

$$B_z(\vec{k}) = \frac{E_s + \omega - E_p}{2} - \frac{K^2}{\omega} - \frac{|\Omega|^2}{2\omega}$$

(18)

V. CHERN NUMBERS IN TWO-DIMENSIONAL SYSTEMS

The first Chern number is a topological number employed to characterize two-dimensional band insulators such as the integer quantum Hall systems, and the direct relation between the Chern number and Hall conductance [28]. Generally, the Chern numbers can be defined for quantum states with two periodic parameters as integral over a two-dimensional compact surface, such as the Brillouin zone, of a fictitious magnetic fields, which is actually the field strengths of the Berry connection [29].

For example, the Chern number assigned to the nth band is defined by

$$c_n = \frac{1}{2\pi i} \int_{T^2} F_{12}(\vec{k}) \mathrm{d}^2 k$$

where n denotes the nth Bloch band, and the Berry connection $A_\mu(\vec{k})(\mu = 1, 2)$ and the associated field strength $F_{12}(\vec{k})$ are given by

$$
\begin{aligned}
A_\mu(\vec{k}) &= \langle \psi_n(\vec{k})|\partial_\mu|\psi_n(\vec{k})\rangle \\
F_{12}(\vec{k}) &= \partial_1 A_2(\vec{k}) - \partial_2 A_1(\vec{k})
\end{aligned}
$$

Here T^2 means the surface of the two-dimensional Brillouin zone, and $|\psi_n(\vec{k})\rangle$ are normalized Bloch wave functions.

In our model, the Effective Hamiltonian H_{eff} is a two-band Hamiltonian which can be written in this form

$$H_{\text{eff}} = \vec{B}(\vec{k}) \cdot \vec{\sigma} = \varepsilon(\mathbf{k})\hat{\mathbf{n}}(\mathbf{k}) \cdot \tilde{\sigma}$$

where $\vec{\sigma} = (\sigma_x, \sigma_y, \sigma_z)$ is a vector of Pauli matrices acting in the sublattice space and $\hat{\mathrm{n}}$ is a three-dimentional unit vector. When $\varepsilon(\mathbf{k}) \neq \mathbf{0}$, π/T for all $\mathbf{k}$, each quasienergy band of the Effective Hamiltonian could be characterized topologically by the first Chern number, that [20]

$$C_\pm = \frac{\pm 1}{4\pi} \int_{\text{FBZ}} \hat{\mathbf{n}} \cdot (\partial_{\mathbf{k_x}}\hat{\mathbf{n}} \times \partial_{\mathbf{k_y}}\hat{\mathbf{n}}) \mathbf{d^2 k}$$

For further study, an efficient method of calculating the Chern numbers on a discretized Brillouin zone could be putted to this model, using the results above.

作者签名：

REFERENCES

[1] M. Z. Hasan, and C. L. Kane, Rev. Mod. Phys. **82**, 3045 (2010).

[2] X.-L. Qi, and S.-C. Zhang, Rev. Mod. Phys. **83**, 1057 (2011).

[3] L. Fu, C. L. Kane, and E. J. Mele, Phys. Rev. Lett. **98**, 106803 (2007).

[4] B. A. Bernevig, T. L. Hughes, and S.-C. Zhang, Science **314**, 1757 (2006).

[5] M. König, S. Wiedmann, C. Brüne, A. Roth, H. Buhmann, L. W. Molenkamp, X.-L. Qi, and S.-C. Zhang, Science **318**, 766 (2007).

[6] D. Hsieh, D. Qian, L. Wray, Y. Xia, Y. S. Hor, R. J. Cava, and M. Z. Hasan, Nature(London) **452**, 970 (2008).

[7] C.-Z. Chang, J. Zhang, X. Feng, J. Shen, Z. Zhang, M. Guo, K. Li, Y. Ou, P. Wei, L.-L. Wang, Z.-Q. Ji, Y. Feng, S. Ji, X. Chen, J. Jia, X. Dai, Z. Fang, S.-C. Zhang, K. He, Y. Wang, L. Lu, X.-C. Ma, and Q.-K. Xue, Science, **340**, 167 (2013).

[8] Y.-J. Lin, R. L. Compton, K. Jiménez-García, J. V. Porto, and I. B. Spielman, Nature(London) **462**, 628 (2009).

[9] Y.-J. Lin, K. Jiménez-García, and I. B. Spielman, Nature(London) **471**, 83 (2011).

[10] P.-J. Wang, Z.-Q. Yu, Z. Fu, J. Miao, L. Huang, S. Chai, H. Zhai, and J. Zhang, Phys. Rev. Lett. **109**, 095301 (2012).

[11] L. W. Cheuk, A. T. Sommer, Z. Hadzibabic, T. Yefsah, W. S. Bakr, and M. W. Zwierlein, Phys. Rev. Lett. **109**, 095302 (2012).

[12] M. Aidelsburger, M. Atala, S. Nascimbéne, S. Trotzky, Y.-A. Chen, and I. Bloch, Phys. Rev. Lett. 107, 255301 (2011).

[13] K. Jiménez-García, L. J. LeBlanc, R. A.Williams,M. C. Beeler, A. R. Perry, and I. B. Spielman, Phys. Rev. Lett. **108**, 225303 (2012).

[14] M. Aidelsburger,M. Atala,M. Lohse, J. T. Barreiro, B. Paredes, and I. Bloch, Phys. Rev. Lett. **111**, 185301 (2013).

[15] H. Miyake, G. A. Siviloglou, C. J. Kennedy, W. Cody Burton, and W. Ketterle, Phys. Rev. Lett. **111**, 185302 (2013).

[16] J. Struck, Ölschläger, R. Le Targat, P. Soltan-Panahi, A. Eckardt, M. Lewenstein, P.Windpassinger, andK. Sengstock, Science **333**, 996 (2011).

[17] J. Struck, Ölschläger, M. Weinberg, P. Hauke, J. Simonet, A. Eckardt, M. Lewenstein, K. Sengstock, and P.Windpassinger, Phys. Rev. Lett. **108**, 225304 (2012).

[18] C. V. Parker, L. C. Ha, and C. Chin, Nat. Phys. **9**, 769 (2013).

[19] Di Xiao, M.-C. Chang, and Q. Niu, Rev. Mod. Phys. **82** (1959).

[20] Takuya Kitagawa, Erez Berg, Mark Rudner, and Eugene Demler, Phys. Rev. B **82**, 235114 (2010).

[21] M. S. Rudner, N. H. Lindner, E. Berg, M. Levin, Phys. Rev. X **3**, 031005 (2013).

[22] N. Goldman, and J. Dalibard, Phys. Rev. X **4**, 031027 (2014).

[23] W. Zheng, and H. Zhai, Phys. Rev. A **89**, 061603(R) (2014).

[24] S.-L. Zhang, and Qi Zhou, Phys. Rev. A **90**, 051601(R) (2014).

[25] J. H. Shirley, Phys. Rev. **138**, B979 (1965).

[26] G. Jotzu, M. Messer, R. Desbuquois, M. Lebrat, T. Uehlinger, D. Greif, and T. Esslinger Nature(London) **515**, 237 (2014).

[27] S. Rahav, I. Gilary, and S. Fishman, Phys. Rev. A **68**, 013820 (2003).

[28] D. J. Thouless, M. Kohmoto, M. P. Nightingale, and M. den Nijs, Phys. Rev. Lett. **49**, 405 (1982).

[29] T. Fukui, Y. Hatsugai, and H. Suzuki, J. Phys. Soc. Jpn. **74**, 1674 (2005).

APPENDICES

Appendix A.   EFFECTIVE HAMILTONIAN CORRESPONDING TO A FLOQUET OPERATOR

Suppose our system is subjected to a periodically varying, time-dependent Hamiltonian $H(t) = H(t + T)$. Here T is the period of the driving cycle. The behavior of the system is analyzed in terms of an Floquet operator [25] which is the evolution operator of the system over one full period of the driving, $U(t)$, defined as

$$U(t) = \mathcal{T} e^{-i \int_0^T H(t) \mathrm{d}t}$$

where the $\mathcal{T}$ is the time-ordering operator.

One method to study such a periodically driving system is to introduce a time-independent effective Hamiltonian $\hat{H}_{\text{eff}}$ via $\hat{F} = e^{-i\hat{H}_{\text{eff}}T}$ [27]. Expanding $\hat{H}(t)$ as $\hat{H}(t) = \sum_{n=-\infty}^{\infty} \hat{H}_n(t) e^{in\omega t}$ with $\omega = 2\pi/T$, and for a situation that the static component $\hat{H}_0$ contains energy bands within an energy range of Δ and $\omega \gg \Delta$, it is straightforward to show that to the leading order of Δ/ω, the effective Hamiltonian $\hat{H}_{\text{eff}}$ could be deduced as [27]

$$\hat{H}_{\text{eff}} = \hat{H}_0 + \sum_{n=1}^{\infty} \left(\frac{[\hat{H}_n, \hat{H}_{-n}]}{n\omega} - \frac{[\hat{H}_n, \hat{H}_0]}{e^{-2\pi n i \alpha} n\omega} + \frac{[\hat{H}_{-n}, \hat{H}_0]}{e^{2\pi n i \alpha} n\omega} \right)$$

Here we give an simple deduction. Expanding $U(t)$ to T order, that

$$
\begin{aligned}
U(t) &= \lim_{N \to \infty} \prod_{j=0}^{N} e^{-iH(t_j)\delta t} \\
&= \lim_{N \to \infty} \prod_{j=0}^{N} (1 - iH(t_j)\delta t) \\
&= \lim_{N \to \infty} \prod_{j=0}^{N} \left[1 - i\Delta t \sum_{j=0}^{N} H(t_j) + (-i\Delta t)^2 \sum_{j>k}^{N} H(t_j)H(t_k) + \cdots \right] \\
&= 1 - i \int_0^T \mathrm{d}t H(t) + (-i)^2 \int_0^T \mathrm{d}t_1 \int_0^{t_1} H(t_1)H(t_2) + \cdots
\end{aligned}
$$

Comparing coefficients, we obtain

$$H_{\text{eff}} = H_0 + \frac{1}{\hbar\omega} \sum_{n>0} \frac{1}{n} \left(e^{i\eta n\pi} [H_0, H_n] - e^{-i\eta n\pi} [H_0, H_{-n}] + [H_n, H_{-n}] \right) + O\left(\frac{1}{\omega^2}\right)$$

Appendix B.   MATLAB CODE

B – 1.   Energy Bands Solving and Plotting

i   Energy Bands Solving

```
%% Energy Bands Solving
tic

global eigenzhi % eigenshi

eigenzhi=zeros(2*n-1,2*n-1,(2*n1+1)*(2*n2+1));
% eigenshi=zeros(2*n-1,2*n-1,(2*n1+1)*(2*n2+1),(2*n1+1)*(2*n2+1));

for count_qx=1:2*n-1
    for count_qy=1:2*n-1
        eigenzhi(count_qy,count_qx,:)=...
            OpticalLattice2D_evals...
                (k1,k2,alpha,V1,V2,n1,n2,qxx(count_qx),qyy(count_qy));
    end
end
time_evalsonly=toc
clear qx qy count_qx count_qy time_evalsonly

%% Saving Variables
load('evals+[V=16.0]+[n=500].mat');
evals16=eigenzhi(:,:,1:5);
save evals16.mat evals16
clear all
```

ii   Plotting Energy Bands

```
%% Loading DATA

load('evals16.mat');
eigenzhi=evals16;

%% Plotting a single Energy Band

figure
surf(qxx(:),qyy(:),eigenzhi(:,:,1));
xlabel('k_x/k_1');
ylabel('k_y/k_2');
zlabel('E^{(1)}(k)/\epsilon_0');
shading interp;
% hold on;
```

```
figure
surf(qxx(:),qyy(:),eigenzhi(:,:,2));
xlabel('k_x/k_1');
ylabel('k_y/k_2');
zlabel('E^{(2)}(k)/\epsilon_0');
shading interp;
% hold on;
%%
figure
surf(qxx(:),qyy(:),eigenzhi(:,:,3));
xlabel('k_x/k_1');
ylabel('k_y/k_2');
zlabel('E^{(3)}(k)/\epsilon_0');
shading interp;
% hold on;

%% Plotting Energy Bands
figure
surf(qxx(:),qyy(:),eigenzhi(:,:,1));
hold on;
surf(qxx(:),qyy(:),eigenzhi(:,:,2));
hold on;
surf(qxx(:),qyy(:),eigenzhi(:,:,3));
hold on;
surf(qxx(:),qyy(:),eigenzhi(:,:,4));
hold on;
xlabel('k_x/k_1');
ylabel('k_y/k_2');
zlabel('E^{(i)}(k)/\epsilon_0');

shading interp;
```

B – 2.   Numerical Diagonalization Solving for Bloch Functions

i   Calculating Bloch functions

```
%%  2D Optical Lattice Bloch Functions
tic

clear

global k1 k2 alpha V1 V2 n1 n2 n qxx qyy

k1=1.0;
k2=1.0;
```

```
V1=-16.0;
V2=-16.0;
alpha=-pi/6;
n1=5;
n2=5;
n=50;


qxx=-k1+(1.0/n)*k1:(1.0/n)*k1:k1-(1.0/n)*k1;
qyy=-k2+(1.0/n)*k2:(1.0/n)*k2:k2-(1.0/n)*k2;


time_declaring=toc

clear count_qxy time_declaring;



%% Calculation of EigenValue & EigenFunction(under Bloch bases)
tic

global eigenzhi eigenshi



V=zeros((2*n1+1)*(2*n2+1),(2*n1+1)*(2*n2+1));
D=zeros((2*n1+1)*(2*n2+1),(2*n1+1)*(2*n2+1));

eigenzhi=zeros(2*n-1,2*n-1,(2*n1+1)*(2*n2+1));
eigenshi=zeros(2*n-1,2*n-1,(2*n1+1)*(2*n2+1),(2*n1+1)*(2*n2+1));

for count_qx=1:2*n-1
    for count_qy=1:2*n-1
        [V,D]=OpticalLattice2D_eigH...
            (k1,k2,alpha,V1,V2,n1,n2,qxx(count_qx),qyy(count_qy));
        eigenzhi(count_qy,count_qx,:)=diag(D);
        eigenshi(count_qy,count_qx,:,:)=V;
    end
end

clear V D qx qy ia ib count_qx count_qy

time_bloch=toc
```

B – 3. First Brillouin Zone

```
%% Boundary of First Brillouin  Zone

lineup1=@(x) sqrt(3.0)*x+2.0;
```

```
lineup2=@(x) (-2.0+sqrt(3.0))*(x-2.0);


linedown1=@(x) (-2.0+sqrt(3.0))*(x+2.0);
linedown2=@(x) sqrt(3.0)*x-2.0;

%% First Brillioun Zone Plotting

x=linspace(-2.0,2.0);
figure
plot(x,lineup1(x),'--',x,lineup2(x),':',x,linedown1(x),x,linedown2(x),'c*')
xlim([-1.0,1.0])
ylim([-1.0,1.0])


%% Cutting off Beyond-fbz
tic

for count_qx=1:2*n-1
    for count_qy=1:2*n-1
        if qyy(count_qy)<lineup1(qxx(count_qx))...
                &&qyy(count_qy)<lineup2(qxx(count_qx))...
                &&qyy(count_qy)>linedown1(qxx(count_qx))...
                &&qyy(count_qy)>linedown2(qxx(count_qx))
        else
            eigenzhi(count_qy,count_qx,:)=NaN;
        end
    end
end

time_Cutting_off_Beyond_fbz=toc
```

B – 4.   Phase Locking

This method considers only the five biggest-coefficients bases[4] as a representation for the main part of the Bloch functions to judge if Bloch functions of two next nearing quasi-momentum in Brillouin Zone are differs from an unfixed arbitrary phase. And this part of program is design to lock the arbitrary phase through the whole First Brillouin Zone.

```
%%
global bloch1234

bloch1234=eigenshi(:,:,:,[1,2,3,4]);

blochcoe=bloch1234(:,:,:,1);
```

---

[4]This method is only valid for the lowest four bands. To make it available for more bands, more plain-wave bases needs considering.

```
%% Phase Locking - considering the main part of Bloch function

tic

% nband=2;

lmid=((2*n2+1)*(2*n2+1)+1)/2;
lmid1=lmid-(2*n2+1);
lmid11=lmid+(2*n2+1);
lmid2=lmid-1;
lmid22=lmid+1;

xrange=2.0*(pi/k1);
yrange=2.0*(pi/k2);

global blochcoe

% blochcoe=zeros(2*n-1,2*n-1,(2*n1+1)*(2*n2+1));

for nband=1:4

blochcoe(:,:,:)=eigenshi(:,:,:,nband);

if eigenshi(n,n,lmid,nband)<0
    blochcoe(n,n,:)=-1.0*eigenshi(n,n,:,nband);
end

count_qy=n;
qy=qyy(count_qy);
for count_qx=n-1:-1:1
    qx=qxx(count_qx);
    blochmain=@(x,y) eigenshi(count_qy,count_qx,lmid,nband)...
        .*exp(1i.*(qx.*x+qy.*y))...
        +eigenshi(count_qy,count_qx,lmid1,nband)...
        .*exp(1i.*((2*k1+qx).*x+qy.*y))...
        +eigenshi(count_qy,count_qx,lmid11,nband)...
        .*exp(1i.*((-2*k1+qx).*x+qy.*y))...
        +eigenshi(count_qy,count_qx,lmid2,nband)...
        .*exp(1i.*((2*k2*cos(alpha)+qx).*x+(2*k2*sin(alpha)+qy).*y))...
        +eigenshi(count_qy,count_qx,lmid22,nband)...
        .*exp(1i.*((-2*k2*cos(alpha)+qx).*x+(-2*k2*sin(alpha)+qy).*y));
    qxf=qxx(count_qx+1);
    blochmainf=@(x,y) blochcoe(count_qy,count_qx+1,lmid)...
        .*exp(1i.*(qxf.*x+qy.*y))...
        +blochcoe(count_qy,count_qx+1,lmid1)...
        .*exp(1i.*((2*k1+qxf).*x+qy.*y))...
        +blochcoe(count_qy,count_qx+1,lmid11)...
```

```
        .*exp(1i.*((-2*k1+qxf).*x+qy.*y))...
        +blochcoe(count_qy,count_qx+1,lmid2)...
        .*exp(1i.*((2*k2*cos(alpha)+qxf).*x+(2*k2*sin(alpha)+qy).*y))...
        +blochcoe(count_qy,count_qx+1,lmid22)...
        .*exp(1i.*((-2*k2*cos(alpha)+qxf).*x+(-2*k2*sin(alpha)+qy).*y));
    diffbm=@(x,y) blochmain(x,y)-blochmainf(x,y);
    diffbminv=@(x,y) -blochmain(x,y)-blochmainf(x,y);
    db=quad2d(@(x,y) ...
        conj(diffbm(x,y))...
        .*diffbm(x,y),-xrange,xrange,-yrange,yrange);
    dbinv=quad2d(@(x,y) ...
        conj(diffbminv(x,y))...
        .*diffbminv(x,y),-xrange,xrange,-yrange,yrange);
%     diffbloch(count_qx,1)=db;
%     diffbloch(count_qx,2)=dbinv;
    if abs(db)>abs(dbinv)
        blochcoe(count_qy,count_qx,:)=...
            -1.0*eigenshi(count_qy,count_qx,:,nband);
    end
%     clear blochmain blochmainf diffbm diffbminv db dbinv diffbloch
end
for count_qx=n+1:2*n-1
    qx=qxx(count_qx);
    blochmain=@(x,y) eigenshi(count_qy,count_qx,lmid,nband)...
        .*exp(1i.*(qx.*x+qy.*y))...
        +eigenshi(count_qy,count_qx,lmid1,nband)...
        .*exp(1i.*((2*k1+qx).*x+qy.*y))...
        +eigenshi(count_qy,count_qx,lmid11,nband)...
        .*exp(1i.*((-2*k1+qx).*x+qy.*y))...
        +eigenshi(count_qy,count_qx,lmid2,nband)...
        .*exp(1i.*((2*k2*cos(alpha)+qx).*x+(2*k2*sin(alpha)+qy).*y))...
        +eigenshi(count_qy,count_qx,lmid22,nband)...
        .*exp(1i.*((-2*k2*cos(alpha)+qx).*x+(-2*k2*sin(alpha)+qy).*y));
    qxf=qxx(count_qx-1);
    blochmainf=@(x,y) blochcoe(count_qy,count_qx-1,lmid)...
        .*exp(1i.*(qxf.*x+qy.*y))...
        +blochcoe(count_qy,count_qx-1,lmid1)...
        .*exp(1i.*((2*k1+qxf).*x+qy.*y))...
        +blochcoe(count_qy,count_qx-1,lmid11)...
        .*exp(1i.*((-2*k1+qxf).*x+qy.*y))...
        +blochcoe(count_qy,count_qx-1,lmid2)...
        .*exp(1i.*((2*k2*cos(alpha)+qxf).*x+(2*k2*sin(alpha)+qy).*y))...
        +blochcoe(count_qy,count_qx-1,lmid22)...
        .*exp(1i.*((-2*k2*cos(alpha)+qxf).*x+(-2*k2*sin(alpha)+qy).*y));
    diffbm=@(x,y) blochmain(x,y)-blochmainf(x,y);
    diffbminv=@(x,y) -blochmain(x,y)-blochmainf(x,y);
    db=quad2d(@(x,y)
```

```
        conj(diffbm(x,y))...
        .*diffbm(x,y),-xrange,xrange,-yrange,yrange);
    dbinv=quad2d(@(x,y) ...
        conj(diffbminv(x,y))...
        .*diffbminv(x,y),-xrange,xrange,-yrange,yrange);
    if abs(db)>abs(dbinv)
        blochcoe(count_qy,count_qx,:)=...
            -1.0*eigenshi(count_qy,count_qx,:,nband);
    end
end
end

for count_qx=1:2*n-1
    qx=qxx(count_qx);
    for count_qy=n-1:-1:1
        qy=qyy(count_qy);
        blochmain=@(x,y) eigenshi(count_qy,count_qx,lmid,nband)...
            .*exp(1i.*(qx.*x+qy.*y))...
            +eigenshi(count_qy,count_qx,lmid1,nband)...
            .*exp(1i.*((2*k1+qx).*x+qy.*y))...
            +eigenshi(count_qy,count_qx,lmid11,nband)...
            .*exp(1i.*((-2*k1+qx).*x+qy.*y))...
            +eigenshi(count_qy,count_qx,lmid2,nband)...
            .*exp(1i.*((2*k2*cos(alpha)+qx).*x+(2*k2*sin(alpha)+qy).*y))...
            +eigenshi(count_qy,count_qx,lmid22,nband)...
            .*exp(1i.*((-2*k2*cos(alpha)+qx).*x+(-2*k2*sin(alpha)+qy).*y));
        qyf=qyy(count_qy+1);
        blochmainf=@(x,y) blochcoe(count_qy+1,count_qx,lmid)...
            .*exp(1i.*(qx.*x+qyf.*y))...
            +blochcoe(count_qy+1,count_qx,lmid1)...
            .*exp(1i.*((2*k1+qx).*x+qyf.*y))...
            +blochcoe(count_qy+1,count_qx,lmid11)...
            .*exp(1i.*((-2*k1+qx).*x+qyf.*y))...
            +blochcoe(count_qy+1,count_qx,lmid2)...
            .*exp(1i.*((2*k2*cos(alpha)+qx).*x+(2*k2*sin(alpha)+qyf).*y))...
            +blochcoe(count_qy+1,count_qx,lmid22)...
            .*exp(1i.*((-2*k2*cos(alpha)+qx).*x+(-2*k2*sin(alpha)+qyf).*y));
        diffbm=@(x,y) blochmain(x,y)-blochmainf(x,y);
        diffbminv=@(x,y) -blochmain(x,y)-blochmainf(x,y);
        db=quad2d(@(x,y) ...
            conj(diffbm(x,y)).*diffbm(x,y),-xrange,xrange,-yrange,yrange);
        dbinv=quad2d(@(x,y) ...
            conj(diffbminv(x,y)).*diffbminv(x,y),-xrange,xrange,-yrange,yrange);
        if abs(db)>abs(dbinv)
            blochcoe(count_qy,count_qx,:)=...
                -1.0*eigenshi(count_qy,count_qx,:,nband);
        end
    end
end
```

```matlab
    for count_qy=n+1:2*n-1
        qy=qyy(count_qy);
        blochmain=@(x,y) eigenshi(count_qy,count_qx,lmid,nband)...
            .*exp(1i.*(qx.*x+qy.*y))...
            +eigenshi(count_qy,count_qx,lmid1,nband)...
            .*exp(1i.*((2*k1+qx).*x+qy.*y))...
            +eigenshi(count_qy,count_qx,lmid11,nband)...
            .*exp(1i.*((-2*k1+qx).*x+qy.*y))...
            +eigenshi(count_qy,count_qx,lmid2,nband)...
            .*exp(1i.*((2*k2*cos(alpha)+qx).*x+(2*k2*sin(alpha)+qy).*y))...
            +eigenshi(count_qy,count_qx,lmid22,nband)...
            .*exp(1i.*((-2*k2*cos(alpha)+qx).*x+(-2*k2*sin(alpha)+qy).*y));
        qyf=qyy(count_qy-1);
        blochmainf=@(x,y) blochcoe(count_qy-1,count_qx,lmid)...
            .*exp(1i.*(qx.*x+qyf.*y))...
            +blochcoe(count_qy-1,count_qx,lmid1)...
            .*exp(1i.*((2*k1+qx).*x+qyf.*y))...
            +blochcoe(count_qy-1,count_qx,lmid11)...
            .*exp(1i.*((-2*k1+qx).*x+qyf.*y))...
            +blochcoe(count_qy-1,count_qx,lmid2)...
            .*exp(1i.*((2*k2*cos(alpha)+qx).*x+(2*k2*sin(alpha)+qyf).*y))...
            +blochcoe(count_qy-1,count_qx,lmid22)...
            .*exp(1i.*((-2*k2*cos(alpha)+qx).*x+(-2*k2*sin(alpha)+qyf).*y));
        diffbm=@(x,y) blochmain(x,y)-blochmainf(x,y);
        diffbminv=@(x,y) -blochmain(x,y)-blochmainf(x,y);
        db=quad2d(@(x,y) ...
            conj(diffbm(x,y)).*diffbm(x,y),-xrange,xrange,-yrange,yrange);
        dbinv=quad2d(@(x,y) ...
            conj(diffbminv(x,y)).*diffbminv(x,y),-xrange,xrange,-yrange,yrange);
        if abs(db)>abs(dbinv)
            blochcoe(count_qy,count_qx,:)=...
                -1.0*eigenshi(count_qy,count_qx,:,nband);
        end
    end
end

bloch1234(:,:,:,nband)=blochcoe;

end

save bloch1234.mat bloch1234

time_phaselocking=toc
```

B – 5. Wannier Functions

i Fourier transform to obtain Wannier functions

```
%% Wannier Functions Calculations based on Bloch functions above

tic

nband=1;
nn=0;
wann=0.0;

% nsig=((-1)^nband+1)/2;

% wannier=@(x,y) 0.0;

% wannier=Wannier_func(x,y,nband,edge1_index,edge2_index)

xrange=2.0*(pi/k1);%*cos(alpha);
yrange=2.0*(pi/k2);

[x,y]=meshgrid(-xrange:xrange/100:xrange,-yrange:yrange/100:yrange);




for count_qx=1:2*n-1
    qx=qxx(count_qx);
    for count_qy=1:2*n-1
        qy=qyy(count_qy);
        if (qy<lineup1(qx))&&(qy<lineup2(qx))&&...
                (qy>linedown1(qx))&&(qy>linedown2(qx))
            for cl1=1:2*n1+1
                l1=-n1+cl1-1;
                for cl2=1:2*n2+1
                    l2=-n2+cl2-2;
                    wann=wann...
                        +blochcoe(count_qy,count_qx,(cl1-1)*(2*n2+1)+cl2)...
                        *exp(1i*((qx+2*l1*k1+2*l2*k2*cos(alpha))*x...
                        +(qy+2*l2*k2*sin(alpha))*y));
                end
            end
            nn=nn+1;
        end
    end
end
wann=wann.*(sqrt(k1.*k2.*sin(alpha))./pi)./nn;
% wann=real(wann);
```

```
% wann=conj(wann).*wann;

save wann4[2].mat wann

time_wannier=toc
```

ii Plotting Wannier functions

```
%% Plotting Wannier functions
figure
surf(x,y,real(wann));
shading interp;
xlabel('x(1/k_1)');
ylabel('y(1/k_2)');
zlabel('w4(x,y)-real');
xlim([-2.0*(pi/k1) 2.0*(pi/k1)]);
ylim([-2.0*(pi/k2) 2.0*(pi/k2)]);

figure
surf(x,y,imag(wann));
shading interp;
xlabel('x(1/k_1)');
ylabel('y(1/k_2)');
zlabel('w4(x,y)-imag');
xlim([-2.0*(pi/k1) 2.0*(pi/k1)]);
ylim([-2.0*(pi/k2) 2.0*(pi/k2)]);

figure
surf(x,y,conj(wann).*wann);
shading interp;
xlabel('x(1/k_1)');
ylabel('y(1/k_2)');
zlabel('w4(x,y)-abs2');
xlim([-2.0*(pi/k1) 2.0*(pi/k1)]);
ylim([-2.0*(pi/k2) 2.0*(pi/k2)]);

clear x y time_wannier count_qx count_qy cl1 cl2 l1 l2 nn
```

B – 6.   Functions Called by the Main Program

i OpticalLattice2D_evals.m

```
function evals=OpticalLattice2D_evals(k1,k2,alpha,V1,V2,n1,n2,qx,qy)

%$$$$$ taken e0=hbar^2k0^2/2miu as ebergy unit $$$$$
```

```matlab
H=zeros((2*n1+1)*(2*n2+1),(2*n1+1)*(2*n2+1));

qsquare=qx^2+qy^2;


for i=1:2*n1+1
    for j=1:2*n1+1
        for ii=1:2*n2+1
            for jj=1:2*n2+1
                if(i==j)&&(ii==jj)
                    l1=-n1+j-1;
                    l2=-n2+jj-1;
                       H((i-1)*(2*n2+1)+ii,(j-1)*(2*n2+1)+jj)=...
                            4*l1^2*k1^2+4*l2^2*k2^2+8*l1*l2*k1*k2*cos(alpha)...
                            +qsquare...
                            +4*l1*k1*qx+4*l2*k2*(qx*cos(alpha)+qy*sin(alpha));
                elseif((i==j)&&(ii==jj+1))
                    H((i-1)*(2*n2+1)+ii,(j-1)*(2*n2+1)+jj)=0.5*V2;
                elseif((i==j)&&(ii==jj-1))
                    H((i-1)*(2*n2+1)+ii,(j-1)*(2*n2+1)+jj)=0.5*V2;
                elseif((i==j+1)&&(ii==jj))
                    H((i-1)*(2*n2+1)+ii,(j-1)*(2*n2+1)+jj)=0.5*V1;
                elseif((i==j-1)&&(ii==jj))
                    H((i-1)*(2*n2+1)+ii,(j-1)*(2*n2+1)+jj)=0.5*V1;
                end
            end
        end
    end
end

evals=eig(H);

end
```

ii   OpticalLattice2D_eigH.m

```matlab
function[V,D]=OpticalLattice2D_eigH(k1,k2,alpha,V1,V2,n1,n2,qx,qy)
%$$$$$ taken e0=hbar^2k0^2/2miu as ebergy unit $$$$$


H=zeros((2*n1+1)*(2*n2+1),(2*n1+1)*(2*n2+1));

qsquare=qx^2+qy^2;
```

```
for i=1:2*n1+1
    for j=1:2*n1+1
        for ii=1:2*n2+1
            for jj=1:2*n2+1
                if(i==j)&&(ii==jj)
                    l1=-n1+j-1;
                    l2=-n2+jj-1;
                      H((i-1)*(2*n2+1)+ii,(j-1)*(2*n2+1)+jj)=...
                          4*l1^2*k1^2+4*l2^2*k2^2+8*l1*l2*k1*k2*cos(alpha)...
                          +qsquare...
                          +4*l1*k1*qx+4*l2*k2*(qx*cos(alpha)+qy*sin(alpha));
                elseif((i==j)&&(ii==jj+1))
                    H((i-1)*(2*n2+1)+ii,(j-1)*(2*n2+1)+jj)=0.5*V2;
                elseif((i==j)&&(ii==jj-1))
                    H((i-1)*(2*n2+1)+ii,(j-1)*(2*n2+1)+jj)=0.5*V2;
                elseif((i==j+1)&&(ii==jj))
                    H((i-1)*(2*n2+1)+ii,(j-1)*(2*n2+1)+jj)=0.5*V1;
                elseif((i==j-1)&&(ii==jj))
                    H((i-1)*(2*n2+1)+ii,(j-1)*(2*n2+1)+jj)=0.5*V1;
                end
            end
        end
    end
end

[V,D]=eig(H);

% [V,D]=eigs(H,(2*n1+1)*(2*n2+1));


end
```